Design of a cost-effective photogrammetric 3D-imaging system for small archaeological artifacts

Optimized for the depth of field

Marcos Alvarez

Report no	: MSD 2021.057
Coach	: Ir. J.W. Spronck
Professor	: Ir. J.W. Spronck
Specialisation	: Mechatronic System Design
Type of report	: Master of Science Thesis
Date	: 6 September 2021

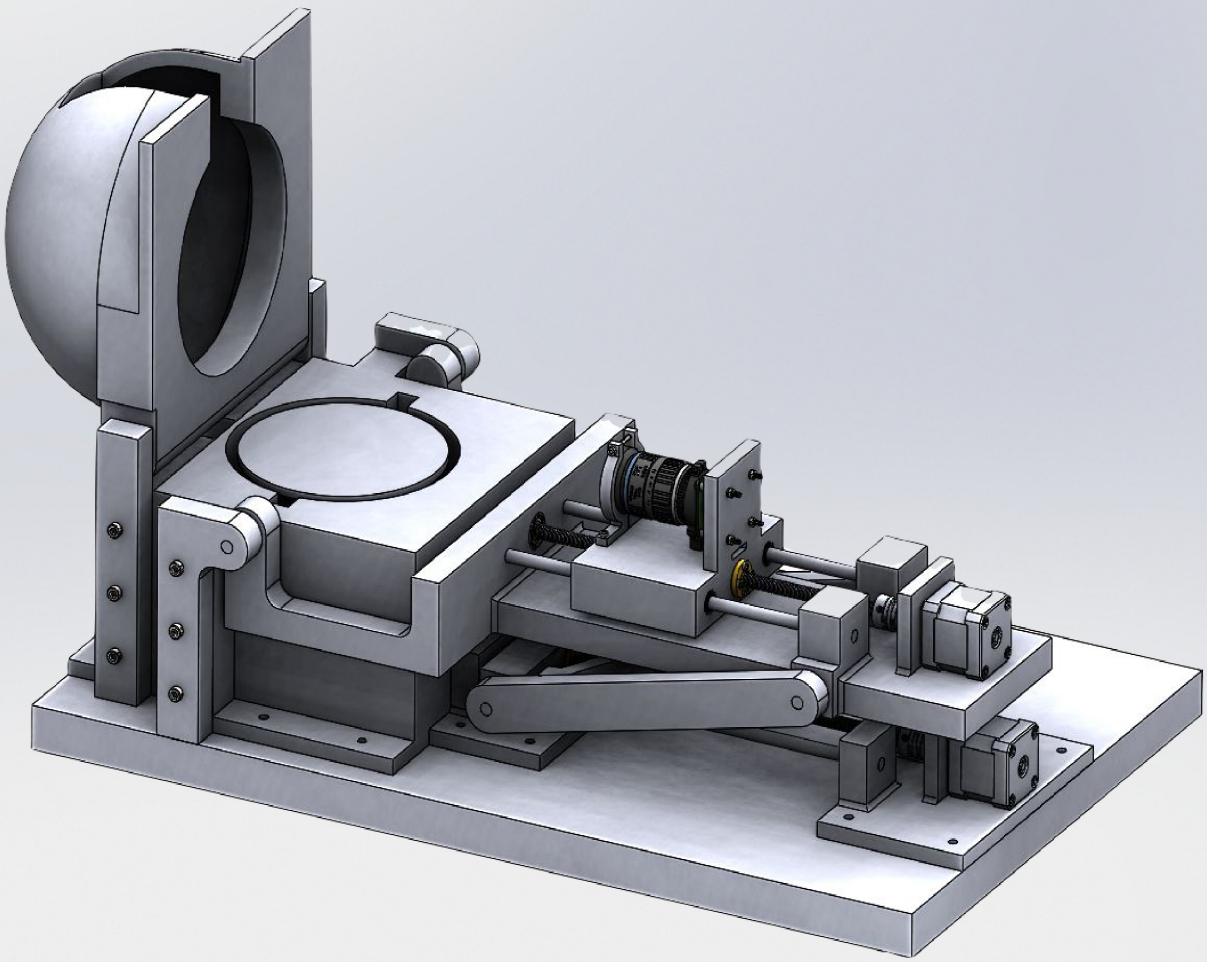

TU Delft Delft University of Technology

Challenge the future

Department of Precision and Microsystems Engineering

Design of a cost-effective photogrammetric 3D-imaging system for small archaeological artifacts

Optimized for the depth of field

by

Marcos Alvarez

to obtain the degree of Master of Science
at the Delft University of Technology,
to be defended publicly on Monday 6 September, 2021 at 13:30 PM.

Student number:	4377923	
Thesis committee:	Ir. J. W. Spronck,	TU Delft, supervisor
	Dr. S. H. HosseinNia,	TU Delft

TU Delft Delft University of Technology

Summary

The 3D-digitisation of precious cultural heritage artifacts is highly important for historical preservation purposes. Doing so can help mitigate against events such as tourism damage, natural disasters, and war. It also enables access to three-dimensional data for researchers of all disciplines all around the globe to study these artifacts. These researchers can study the same object simultaneously without subjecting the fragile original artifacts to the danger of potentially damaging them. Also, future generations can benefit from an online database of archaeological artifacts for educational purposes. Not only that, but the resulting 3D-images can also be used for entertainment purposes, such as video game development, 3D-animations, and virtual reality.

Several high-end solutions are available, but the cost to purchase or leasing can be too substantial for many heritage institutions that often run on small budgets. Currently, several high-end solutions are available to 3D-digitize the archaeological artifacts. One of them is the conveyor system by CultLab3D [21]. It utilizes different 3D-imaging technologies and can create a high-quality 3D-image of archaeological artifacts in a fast way. Although this is a sophisticated solution, the cost to purchase or leasing can be too substantial for many heritage institutions that often run on small budgets [24]. Therefore, there is a need for cost-effective solutions to create 3D-images of small archaeological artifacts. These solutions must be as compact and as automated as possible. There are still millions of artifacts that need to be 3D-digitized. The focus of this thesis will be the digitization of small archaeological artifacts with a length and width ranging between 2 and 5 cm. The reason for this is to have clear requirements for the system, and also, a more compact system can be designed when it is intended to be used for small archaeological artifacts.

When 3D-digitizing small archaeological artifacts, it is important to capture the texture details and preserve color information correctly. Dimensional accuracy is not that important for this application. An extensive literature study was done on the existing 3D-imaging technologies and existing systems. The goal of the literature study was to find the most suitable 3D-imaging technology for this project and to understand what current systems are able to do and what could potentially be improved. The focus of possible improvements was regarding the created quality of the 3D-image, cost, speed, and automation. An overview was created with the advantages and disadvantages of each 3D-imaging technology. It was concluded that photogrammetry is the most suitable 3D-imaging technology available to create high-quality 3D-images of small archaeological artifacts. Photogrammetry is the most suitable because it can be used for small objects, it creates 3D-images with high-quality realistic textures while preserving color information, it can be automated, and it can be cost-effective. Photogrammetry creates digital 3D-images of objects by taking multiple photographs at different angles from the object. These photographs are then used as a data set to implement in the photogrammetry software that creates a 3D-image. The photogrammetry software identifies identical feature points between the different photographs to calculate the distances and creates a 3D-image of the object. The requirements for photogrammetry are that the photographs that will be used as an input for the photogrammetry software are high-resolution, have sufficient depth of field, have good lighting, sufficient angles photographed, and sufficient overlap between the photographs.

Existing photogrammetric systems and available literature have been further studied on the ability to create high-quality 3D-images of small objects in an optimized and cost-effective way. The existing systems offer good results. However, available literature indicates that the results are not optimal due to a small depth of field. When photographing a small object closely, by the nature of optics, the depth of field gets smaller when decreasing the object distance to the camera. As a result of the photographs having a small depth of field, parts of the photograph will be blurry. Because some of the parts of the photograph are blurry, details of the object's texture will not be visible. These photographs will then be used as an input for the photogrammetry software to create a 3D-image of the object. Because the input for the photogrammetry software does not have optimal quality, the resulting 3D-image will

also not be optimal. The quality of the constructed 3D-image is highly dependent on the quality of the photographs.

The small depth of field limitation can be counteracted by a narrow aperture, which cancels out a large portion of the light cone in order to decrease the fall-off in sharpness. But this only works to a certain degree. If the aperture opening becomes too narrow, light waves begin to blend and soften the image. This phenomenon is called diffraction [18]. Also, by narrowing the aperture, the exposure time increases. Therefore, it is desired to use a different technique to extend the depth of field. The depth of field limitations with photogrammetric 3D-imaging systems offers an opportunity to improve existing systems. By extending the depth-of-field of the photographs, high-resolution photographs can be made and used as an input for the photogrammetry software to create a high-quality 3D-image of the object. Extending the depth of field can be achieved by a technique called focus stacking. By photographing the object at different distances from the camera, different parts of the object are in focus. These photographs are then stacked into one high-resolution photograph where the object is visible completely sharp.

The objective of this project was to design a cost-effective photogrammetric 3D-imaging system for small archaeological artifacts. This photogrammetric system is optimized for the depth of field. By using focus stacking, the depth of field of photographs is extended to create high-quality 3D-images of small archaeological artifacts with highly detailed textures and color information. This system must be as automated and compact as possible. The challenges imposed with the stated objective are designing a stable and fast system, creating a good lighting setup, integrating all the subsystems, making the design cost-effective, and optimizing the system. The system is divided into the following subsystems: the photographing subsystem, the positioning subsystem, and the lighting subsystem. For each of these subsystems, choices are made to create a system that satisfies the system requirements. Firstly, a conceptual system is generated, then a detailed system is designed with the necessary calculations and analyses.

A prototype of the designed system was successfully built. To evaluate the system, firstly, an overview of the involved variables that influence the system's performance is given. Separate sub-systems and functions of the system were evaluated. A 3D-image with the best settings was created of an example object, and also a 3D-image was created with minimal settings. Between these two extremes, the variables involved could be tweaked to find an optimum regarding the quality of the 3D-image and the time needed to acquire it. And finally, recommendations are made on how to improve the system. These further improvements aim to create an even faster and more automated system that still can create high-quality 3D-images. The new design can then be further developed and be used by heritage institutions to create high-quality 3D-images of small archaeological artifacts for different important purposes.

Finally, this project can be summarized in the following way. A cost-effective photogrammetric 3D-imaging system for small archaeological artifacts was successfully designed and validated. This system is optimized for the depth of field and is able to successfully create high-quality 3D-images with highly detailed textures and color information, which serves several important purposes. This design overcomes the small depth of field limitations by implementing focus stacking. The system's most intensive task, the acquisition of photographs, has been automated, and a working compact system has been created. The system, as it is, is ready to be used by others. The designed system creates higher-quality 3D-images compared to other cost-effective solutions. Compared to expensive systems, the designed system creates 3D-images of comparable quality. However, the time to acquire the 3D-image with the designed system is significantly longer compared to expensive systems. Figures 1 and 2 show the designed system and a created high-quality 3D-image of a small object.

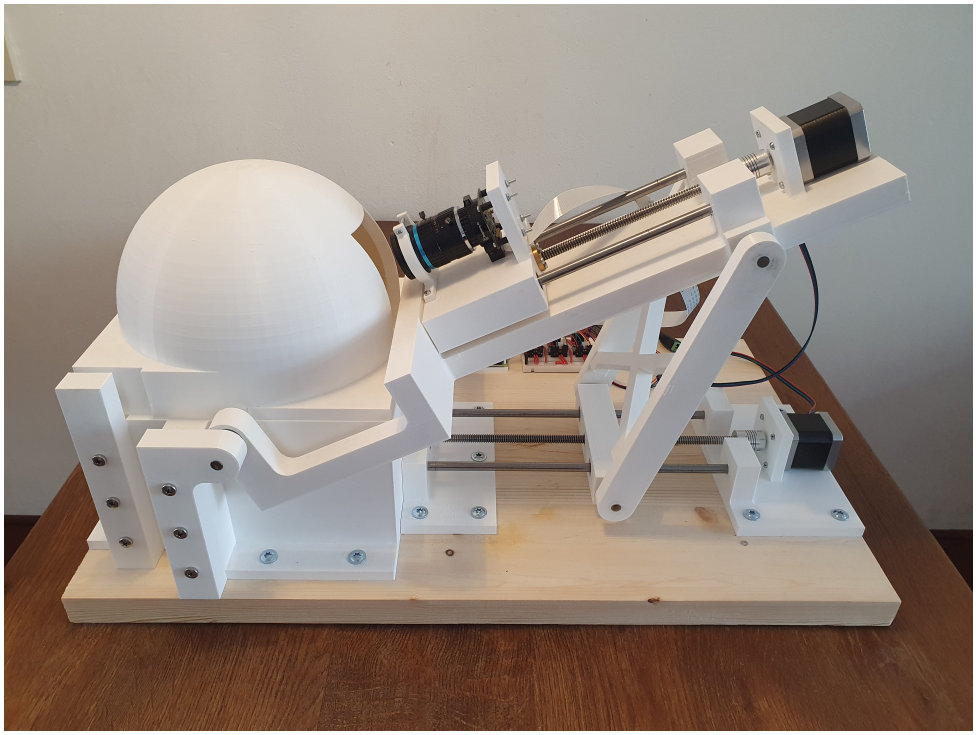

Figure 1: The designed system.

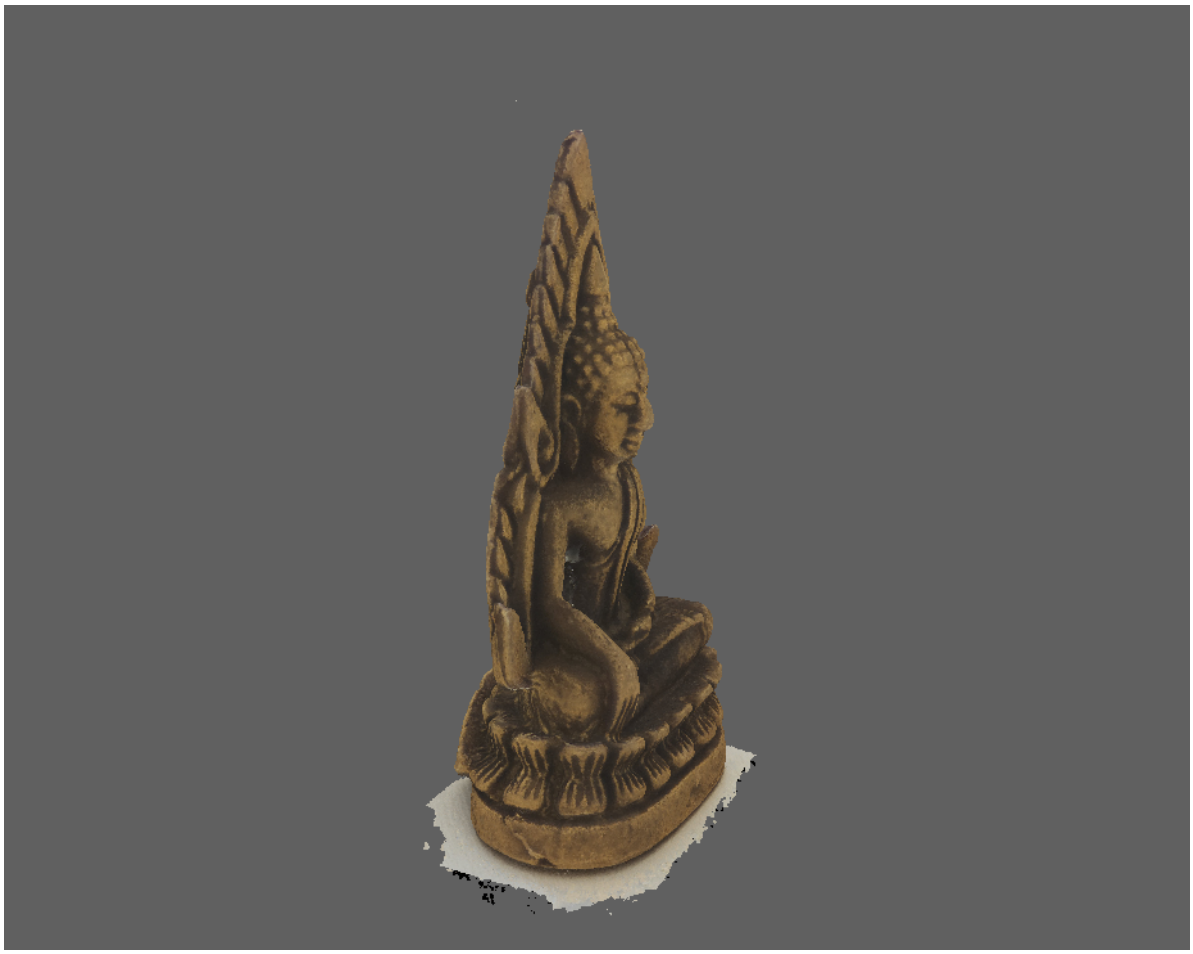

Figure 2: High-quality 3D-image created with the designed system. Click the figure to be able to move the 3D-image.

Preface

In this section, I would like to express my gratitude to everyone who contributed to this project and supported me during my time studying at the TU Delft.

I would like to express my gratitude to my supervisor Ir. J.W. (Jo) Spronck for his guidance throughout my thesis. Thank you for asking me the right questions and improve my system-level thinking.

Thank you, Dr. S. H. (Hassan) HosseinNia, for being part of my thesis committee.

Thank you, fellow students and friends, for the interesting discussions on my project and your projects.

I would like to thank the professors that taught me the courses throughout the years to become a Mechanical Engineer.

Finally, I would like to thank my parents, my family, and my friends. Without your support, this would not have been possible.

Marcos Alvarez
Delft, September 2021

Contents

1 Introduction

In this chapter, 3D-imaging of small archaeological artifacts is introduced. Also, the extensive literature study that has been done on 3D-imaging technologies and 3D-imaging systems is discussed. Next to that, the project objective is stated. And finally, an overview of the thesis is given.

1.1. 3D-Imaging of small archaeological artifacts

The 3D-digitisation of precious cultural heritage artifacts is highly important for historical preservation purposes. Doing so can help mitigate against events such as tourism damage, natural disasters, and war. It also enables worldwide access to three-dimensional data for researchers of all disciplines all around the globe to study these artifacts. These researchers can study the same object simultaneously without subjecting the fragile original artifacts to the danger of potentially damaging them. Also, future generations can benefit from an online database of archaeological artifacts for educational purposes. Not only that, but the resulting 3D-images can also be used for entertainment purposes, such as video game development, 3D-animations, and virtual reality. In Figure 1.1, two examples of archaeological artifacts can be seen.

(a) (b)

Figure 1.1: Two examples of small archaeological artifacts [5]. **(a)** Old jewelry piece. **(b)** Old ring.

Currently, several high-end solutions are available to 3D-digitize the archaeological artifacts. One of them is the conveyor system by CultLab3D [21]. It utilizes different 3D-imaging technologies and can create a high-quality 3D-image of archaeological artifacts in a fast way. Although this is a sophisticated solution, the cost to purchase or leasing can be too substantial for many heritage institutions that often run on small budgets [24]. Therefore, there is a need for cost-effective solutions to create 3D-images

of archaeological artifacts. There are still millions of artifacts that need to be 3D-digitized. For this project, the focus will be on digitizing small archaeological artifacts ranging between 2 and 5 cm. The reason for this is to have clear requirements for the system, and also, a more compact system can be designed when it is intended to be used for small archaeological artifacts.

1.2. Literature study

When 3D-digitizing small archaeological artifacts, it is important to capture the texture details and preserve color information correctly. Dimensional accuracy is not that important for this application. High resolution is important in order to have detailed textures. An extensive literature study was done on the existing 3D-imaging technologies and existing systems. The goal of the literature study was to find the most suitable 3D-imaging technology for this project and to understand what current systems can do and what could potentially be improved. An overview was created with the advantages and disadvantages of each 3D-imaging technology. The literature study can be found in Appendix A. In Figure 1.2 an overview of the 3D-imaging technologies can be seen. It was concluded that photogrammetry is the most suitable 3D-imaging technology available to create high-quality 3D-images of small archaeological artifacts. Photogrammetry is the most suitable because it can be used for small objects, it creates 3D-images with high-quality realistic textures while preserving color information, it can be automated, and it can be cost-effective. Photogrammetry creates digital 3D-images of objects by taking multiple photographs at different angles from the object. These photographs are then used as a data set to implement in the photogrammetry software that creates a 3D-image. The photogrammetry software identifies identical feature points between the different photographs to calculate the distances and creates a 3D-image of the object.

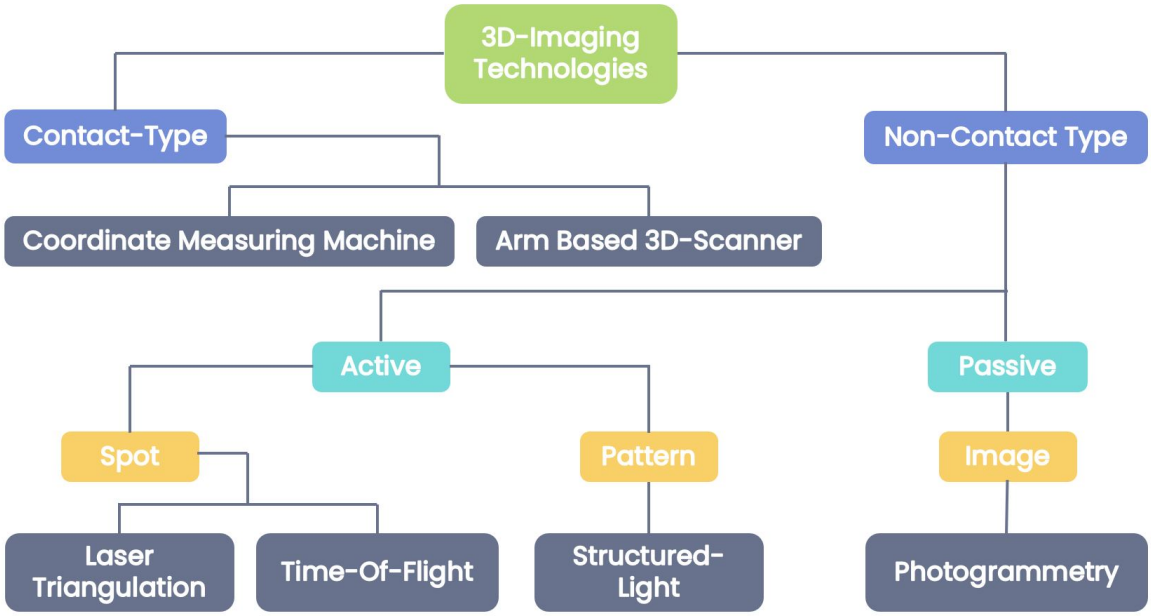

Figure 1.2: Overview of the different 3D-imaging technologies.

A major weakness of photogrammetry is the dependence of a specialized camera operator who can configure the camera parameters and obtain the photographs correctly. If the images are not acquired correctly, subsequent 3D reconstruction will be affected by the presence of significant noise and construction errors [20]. If the process is not automated, it allows for more user error, so the quality of the 3D-image depends greatly on the experience of the operator [11]. Therefore, it is desirable to automate the image acquisition to create an optimal data-set to implement in the photogrammetry software. By automating the acquisition of photographs, high-quality 3D-images of objects can consistently be created. The technology photogrammetry to create 3D-images could, in theory, be utilized just by using the camera of a mobile phone or another camera. The multiple photographs of the object made with this camera by hand can then be used as an input for the photogrammetry. However, achieving this

manually is a hard and time-consuming task, and the results are often not great. Doing this results in inconsistent and low-quality 3D-images. This is because the photogrammetry software has difficulties identifying the identical feature points on the object from the photographs. Making photographs by hand makes it difficult to follow a path without moving the camera too much and still having enough photograph overlap. Therefore, it is desirable to automate the process of making photographs of the object. Also, by having an automated system, archaeologists and researchers with limited knowledge about photography and photogrammetry can still use it.

Existing photogrammetric systems and available literature have been further studied on the ability to create high-quality 3D-images of small objects in an optimized and cost-effective way. The existing systems offer good results. However, available literature indicates that the results are not optimal due to a small depth of field [16]. When photographing a small object closely, by the nature of optics, the depth of field gets smaller when decreasing the object distance to the camera. This can be counteracted by a narrow aperture, which cancels out a large portion of the light cone in order to decrease the fall-off in sharpness. But this only works to a certain degree. If the aperture opening becomes too narrow, light waves begin to blend and soften the image. This phenomenon is called diffraction [18]. Therefore, it is desired to use a different technique to extend the depth of field. As a result of the photographs having a small depth of field, parts of the photograph will be blurry. Because some of the parts of the photograph are blurry, details of the object's texture will not be visible. These photographs will then be used as an input for the photogrammetry software to create a 3D-image of the object. Because the input for the photogrammetry software does not have optimal quality, the resulting 3D-image will also not be optimal. The quality of the constructed 3D-image is highly dependent on the quality of the photographs. Therefore, an opportunity exists to improve existing systems. By extending the depth-of-field of the photographs, high-resolution photographs can be made and used as an input for the photogrammetry software to create a high-quality 3D-image of the object.

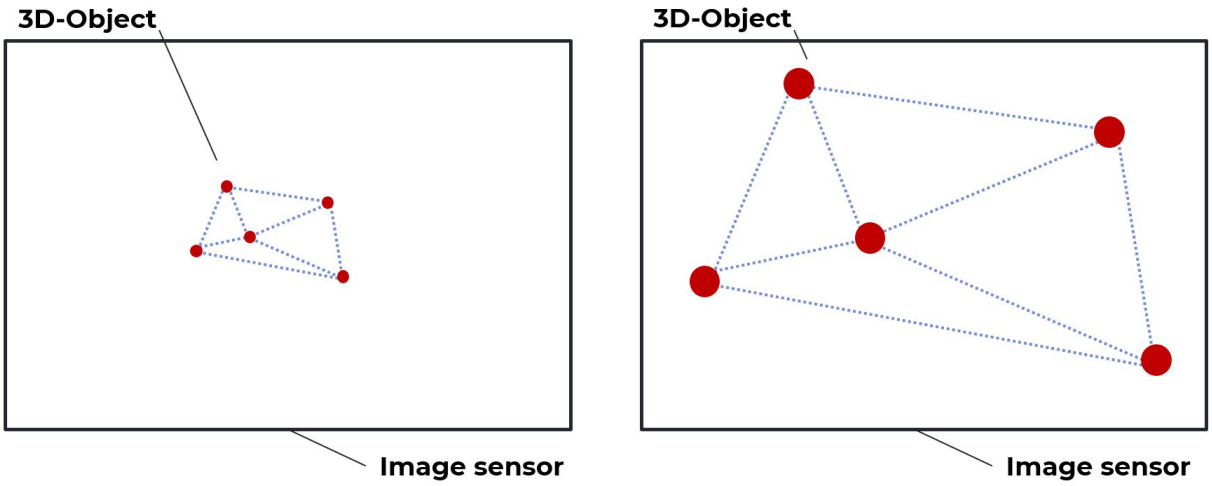

Figure 1.3: Photographing an object at a considerable distance versus photographing an object close (image sensor utilization). When photographing an object at a distance from the camera, the object will be entirely in focus, but the image sensor's resolution will not be optimally utilized. The image sensor will be better utilized by photographing the object closer to the camera, and a higher resolution can be achieved. The downside of doing this is that a shallow depth of field has to be overcome.

The existing devices that can be found in literature take one photo at each angle of the object. There are two reasons why this would not give the best result. The first reason is, by only taking one photo at a close distance, only a specific part of the object is in focus due to a small depth of field. This photo will then be used in the photogrammetry software, and the part of the object that is out of focus will not be modeled with a highly detailed texture in 3D. The second reason is, by taking a photo of the object at a relatively larger distance, the object can be completely in focus, but there is a loss in resolution. This is because the resolution of the image sensor is not completely utilized. This is illustrated in Figure 1.3. A higher-quality 3D-image could be achieved where there is a more detailed texture on the 3D-image. This could be done by solving the small depth of field problem when taking a photo at a close distance relative to the object.

Extending the depth of field can be achieved by a technique called focus stacking. By photographing the object at different distances, different parts of the object are in focus. These photographs are then stacked into one high-resolution image where the object is visible completely sharp. Only one existing system that uses photogrammetry in combination with focus-stacking is available in the literature. They believe they are the first to create such a system, and it was published in 2018 [23]. It is used for creating 3D-images of insects. This setup cannot be used for small archaeological artifacts. A new setup to create 3D-images of small archaeological artifacts will be designed in this study. However, some ideas published in the literature can be extended and used in the proposed new design.

1.3. Project objective

This project aims to design a cost-effective photogrammetric 3D-imaging system for small archaeological artifacts. This system will be optimized for the depth of field. It will extend the depth of field of photographs by using focus stacking to create high-quality 3D-images of small archaeological artifacts with highly detailed textures and color information. In addition, recommendations for the next steps will be made to improve the system even further. The goal of these further improvements is to create an even faster and more automated system that still is able to create high-quality 3D-images. The new design can then be further developed and be used by heritage institutions to create high-quality 3D-images of small archaeological artifacts for different important purposes that have been discussed before.

1.4. Thesis overview

In Chapter 2, focus stacking is explained, which is the technique used to extend the depth of field of the photographs. In Chapter 3, 3D-photogrammetry is further explained, which is the 3D-imaging technology used to create 3D-images of the small archaeological artifacts. The conceptual system design is discussed in Chapter 4, where the system is divided into sub-systems. For these sub-systems, choices are made regarding the needed components to create a conceptual system design. In Chapter 5, the detailed system design is presented with the necessary calculations and considerations for each sub-system and for the complete system. In Chapter 6, the prototype setup is showcased, where the electronics, assembly, and coding are discussed. In Chapter 7, the performance of the prototype setup is evaluated. Finally, in Chapter 8, the conclusions are listed, and recommendations for future work are given. Additionally, multiple appendices are included at the end of the report, where the extensive literature study can be found, the python code used for the prototype setup, and datasheets for components that have been used in this project.

2

Focus stacking explained

This chapter will explain the technique used to extend the depth of field of photographs called focus stacking. Firstly, the working principle of focus stacking will be explained. Secondly, the different focus stacking methods to achieve a focus-stacked image will be discussed. Finally, the focus stacking software that is going to be used for this project will be appointed.

2.1. Working principle

As explained before, photographs that are taken at a close distance to the object are subjected to a shallow depth of field. The depth of field equation is shown below in Equation 2.1, where u is the object distance, f is the focal length of the lens, N is the aperture (f-number), and C is the circle of confusion [28].

$$DOF = \frac{2u^2NC}{f^2} \tag{2.1}$$

The depth of field changes linearly with the f-number and circle of confusion, but it quadratically when changes are made in the focal length and in the distance to the object. As a result, photos taken at highly close range have a proportionally much smaller depth of field. In Figure 2.1, a geometric optical illustration of the photograph formation is depicted. In this illustration, it can be seen that only a part of the object will be in focus. In the depicted illustration, point A of the object will be in focus but points B and C are not. The lens's focal length must be changed, or the lens must be moved accordingly to get either point B or point C in focus. By doing so, the rays converge on the image plane, and the other point is in focus. Focus stacking will be used to overcome the depth of field limitations when photographing an object at a close distance to utilize the resolution of the image sensor.

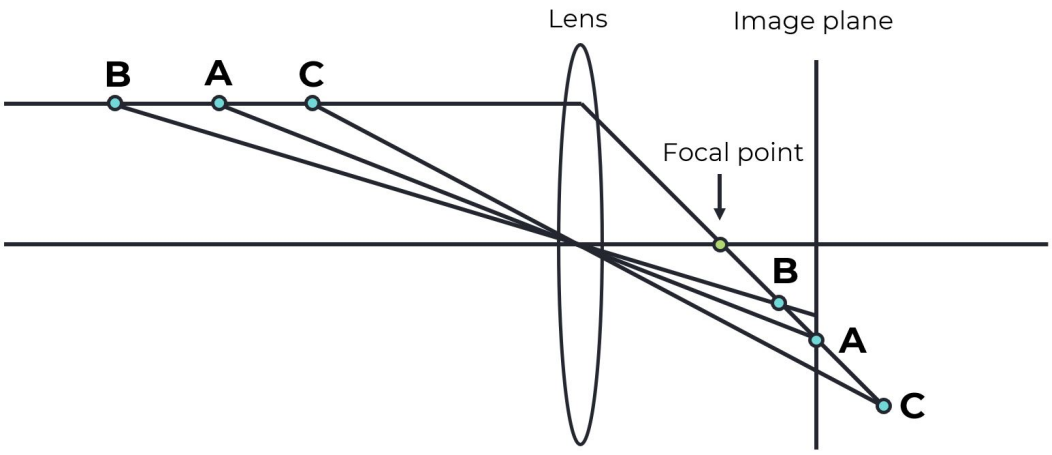

Figure 2.1: A simplified geometric optical illustration of the photograph formation can be seen in this Figure. Point A of the object will be in focus, whereas points B and C will not be in focus in this configuration.

Focus stacking in itself to create a high-resolution image of the object is unnatural because it overcomes the depth of field limitations that happen due to the nature of optics. However, the focus stacking procedure is needed to acquire the best texture details of the object to create a high-quality 3D-image of the object. Focus stacking works in the following way. Several photographs are taken of the object where different parts of the object are in focus. These photographs will be stacked together to create a high-resolution image where all the details of the object are visible. By stacking the photographs together, complementary information from several photographs taken from the same scene is merged to achieve a new focus-stacked image. This stacked image contains the best and all the relevant information from the original photographs. By doing so, the stacked image is of a higher quality compared to all the original photographs.

When the particular photographs are going to be focus-stacked, the following needs to happen. Firstly, for each photograph, the ”best” information of the photograph needs to be identified. Different mathematical operations achieve this, and these will be discussed in subchapter 2.2. The indicators that reflect the region’s amount of information are mainly deviation, and entropy [26]. Secondly, these photographs will be stacked together, containing the best information from each photograph to create a high-resolution image, which is also achieved by mathematical operations. Most of these methods use either pixel-based or region-based stacking methods. The object’s magnification in each photograph changes because the camera is moved or the focal length is changed to take a photograph where another part of the object is in focus. Therefore, in the stacking procedure, the individual photographs have to be scaled and aligned to create a high-quality focus-stacked image. In Figure 2.2, a simplified illustration of the process of focus stacking two photographs to one high-quality image is shown.

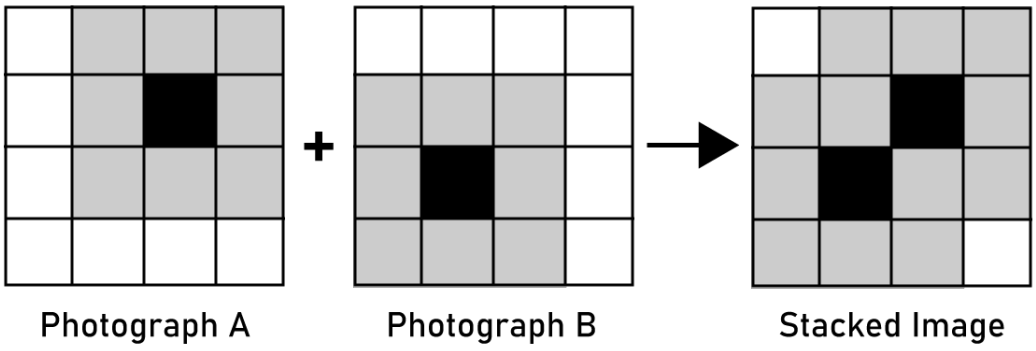

Figure 2.2: A simplified illustration of the focus stacking procedure is shown here. The grey and black area of the images represent the best information that is going to be used for the stacked image to create a high-resolution focus stacked image.

The workflow using focus stacking is depicted in Figure 2.3. For different angles of the object photographs, photographs stacks are created. For these photographs stacks at each angle of the object, a stacked image is created. All the stacked images will then be used as an input for the photogrammetry software to create a high-quality 3D-image.

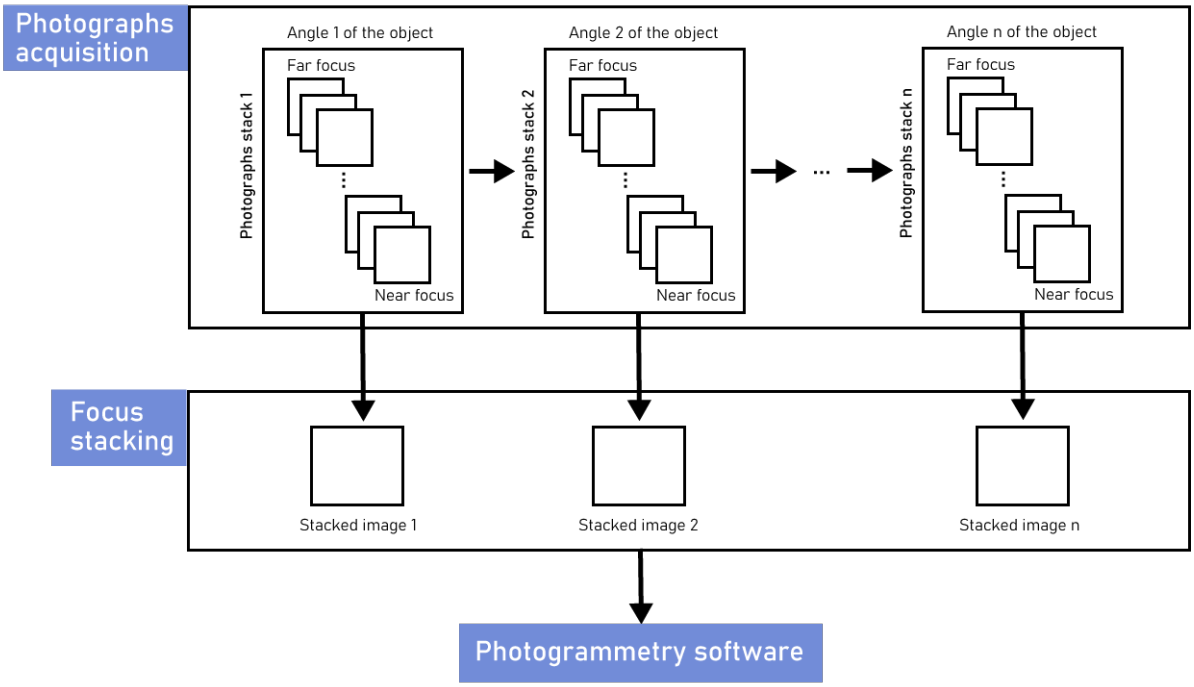

Figure 2.3: In this Figure, the focus stacking workflow is shown. The photographs stacks acquired in the photographs acquisition stage are focus stacked and then implemented in the photogrammetry software.

2.2. Focus stacking methods

Research has been done on the available focus stacking methods to choose the best focus stacking method to create high-quality stacked images. Several different focus stacking methods or image fusion methods include: the weighted-average method, the maximum method, the wavelet transform methods, and the Laplacian pyramid method [26]. These different focus stacking methods utilize different mathematical operations to obtain a focus-stacked image of a set of photographs. These mathematical operations try to identify the relevant and best information of each photograph and try to merge them in the best possible way into one image. The methods mentioned above differ in the quality of the focus-stacked image that they can deliver. According to the paper of Wang et al., which describes the Laplacian pyramid method to create a focus-stacked image, the Laplacian pyramid method provides better results compared to other focus stacking methods in their experimental evaluation [26]. From subjective evaluation, more contrast and more obvious details are visible with the Laplacian pyramid method. From objective evaluation, using quantitative analysis also provides better results with the experiments they have conducted. This project compares different focus stacking methods to verify the conclusion from the found paper that the Laplacian pyramid method provides the best results.

2.3. Software

There is a wide choice of available focus stacking software. The focus stacking software that is going to be used is called **Helicon Focus Pro**. This focus stacking software is well established and known for good quality [9]. The software is simple to use and provides good quality for focus-stacked images. The software has different focus stacking methods available, so comparisons in the quality of the different methods can be made.

3

3D-Photogrammetry explained

In this chapter, 3D-photogrammetry is further explained. The goal is to understand the working principle and map out all the important requirements to use close-range 3D-photogrammetry for small objects optimally. First, the working principle is explained. Secondly, the requirements for 3D-photogrammetry are identified and explained. And finally, the available software and the software that is going to be used are discussed.

3.1. Working principle

As mentioned earlier, 3D-photogrammetry creates digital 3D-images of objects by taking multiple photographs from different angles. These photographs are then used as a data set to implement in 3D-photogrammetry software that creates a 3D-image. The 3D-photogrammetry software identifies identical feature points between the different photographs to calculate the distances and creates a 3D-image of the object. 3D-Photogrammetry is a three-dimensional coordinate measuring technology that uses photographs as the fundamental medium for metrology or measurement. The fundamental principle used in 3D-photogrammetry is triangulation. So-called 'lines of sight' can be developed from each camera position to points on the object. These lines of sight, sometimes called rays owing to their optical nature, are mathematically intersected with software to produce the three-dimensional coordinates of the points of interest [10]. As a result, a digital 3D-image can be constructed from the calculation of the three-dimensional coordinates of the points. In Figure 3.1 this process is depicted. More information on the exact calculations involved in close-range 3D-photogrammetry can be found in the book Close Range Photogrammetry And 3D-Imaging [13].

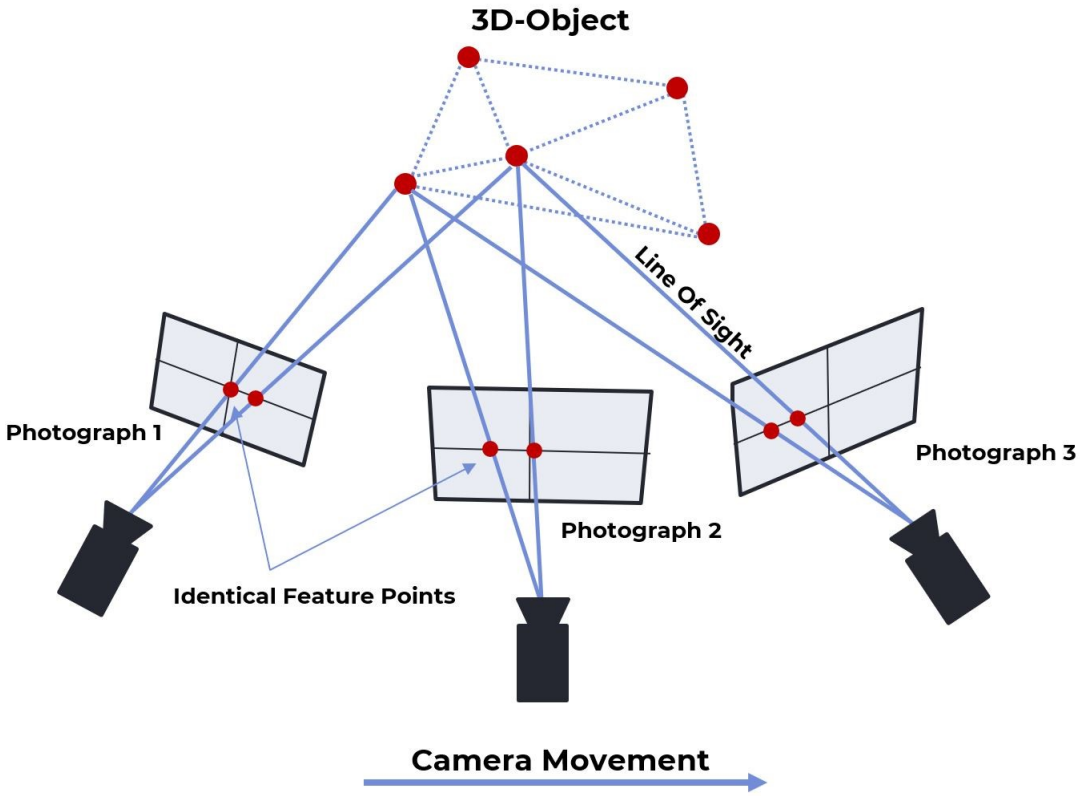

Figure 3.1: In this Figure, the photogrammetric procedure for calculating the shape of the object is shown. By obtaining several photographs of the object, identical feature points can be recognized by the photogrammetry software, and the three-dimensional coordinates of the object can be calculated [25]. Important to note is that the position and orientation of the camera are not critical.

3.2. Requirements for 3D-photogrammetry

The following requirements have to be met to create an optimal data-set of photographs that are going to be used as an input for the 3D-photogrammetry software to create a 3D-image of the small object [13] [3]:

- **High-resolution:** The photographs have to be high-resolution, with the object as much in focus as possible. This is because the resulting 3D-image is very much dependent on the resolution of the photographs. High-resolution photographs are desired to capture the details of the texture as much as possible in the digital 3D-image.
- **Depth of field:** A sufficient depth of field is needed to capture the object completely in focus. Small depth of field results in blurry photographs, diminishing the quality of the 3D-image.
- **Lighting:** Good lighting should be applied to the scene of the object. Good lighting means that no strong shadows and no strong reflections are observed, which could diminish the quality of the 3D-image. Identical feature points are harder for the software to identify when strong shadows and strong reflections are present.
- **Sufficient angles photographed:** The photographs should be taken from a sufficient amount of different angles of the object. This is self-explanatory; it is necessary in order to capture the object completely in the 3D-image. The position and orientation of the camera are not critical.
- **Sufficient overlap between the photographs:** In order for the 3D-photogrammetry software to recognize identical feature points, the photographs should have sufficient overlap.

3.3. Software

3D-Photogrammetry software is available in different forms [4]. 3D- Photogrammetry software exists for long-range photogrammetry and close-range photogrammetry. One example of long-range is aerial 3D-photogrammetry. An example of close-range 3D-photogrammetry is 3D-photogrammetry applied for small objects. Some of the software can create 3D-images for long-range 3D-photogrammetry and close-range 3D-photogrammetry. And some of the software available can only be used for long-range 3D-photogrammetry or close-range 3D-photogrammetry. Although there is a wide variety of 3D-photogrammetry software available with each its strengths and limitations, some of them are popular and used extensively. One of them is Agisoft Metashape, which is highly favored in the highly competitive photogrammetric software industry. Agisoft Metashape is widely used due to its quality, processing time, and reduced complexity which is important for non-experts in 3D-photogrammetry [7]. Therefore, for this project, **Agisoft Metashape** will be used to create 3D-images of small objects using close-range 3D-photogrammetry.

Agisoft Metashape provides additional recommendations to create better results for close-range 3D-photogrammetry for small objects [3]. These recommendations are the following:

- Avoid untextured, highly reflective, and transparent objects. If the scanned surface does not have any distinguishable features, such as irregular color or material texture pattern, the data set will lack reliable information for the reconstruction procedures.
- Regarding ISO, it is recommended to use minimal possible ISO in order to minimize the image noise.
- Use masking tool when processing the photographs:
  - It will help avoid the ghosting effect when generating texture for the model.
  - Save hardware resources thanks to processing only useful data.
  - Allow processing algorithms to work with a meaningful range of data, which is important, for example, when filtering outliers or using a limited number of polygons to reconstruct a mesh model of the scene of interest.
- Controlling the camera movement will help to avoid motion blur.

4

Conceptual system design

In this chapter, the conceptual system design is discussed. With the system is meant the system that will be used to acquire the object's photographs automatically. First, the workflow analysis explaining how the system will be used is presented. Subsequently, the requirements and specifications of the system are explained. Then, the challenges imposed when designing such a system with the listed requirements are considered. Next, the type of components that will be used to design the system are discussed. Furthermore, a conceptual system overview is given. And finally, the concept generation process is explained, and the system choices are substantiated when selecting a concept in the subchapter concept selection.

4.1. Workflow analysis

To understand how the photogrammetric 3D-imaging system will be used, a flowchart that illustrates the workflow is shown in Figure 4.1. The workflow can be divided into two workflow processes: ”photographs acquisition” and ”post-processing”. In the photos acquisition part of the workflow, the necessary photographs of the object will be taken. The user will place the object, and the user will indicate the desired quality of the 3D-image. When choosing a higher quality 3D-image, the process will take longer. When the user presses start, the photographs will start to be made. Multiple photographs will be made at each position that can be focus stacked together to create a high-resolution image. Suppose the bottom part of the object is also relevant for the 3D-image. The bottom part of the object cannot be photographed because it is the part that is lying on a surface so that the object can be photographed. In that case, the user can turn the object and make new photographs of the object in the new position. The user can do this because he or she will be asked if another part of the object should be photographed, and then the process can then be repeated.

In the post-processing part of the workflow, the photographs made at each position are focus stacked. This results in a high-resolution image at each position in which photographs were made. The stacked images are then implemented in the photogrammetry software, and the high-quality 3D-image is created. At the end of the post-processing part of the workflow, the user makes refinements on the 3D-image in the photogrammetry software. This is to remove irrelevant information from the 3D scene, such as background elements, to remain with a clean, high-quality 3D-image.

Therefore, by analyzing the workflow of the system, it can be concluded that it will be a semi-automatic process where the user has to be involved minimally to place the object, to turn over the object if necessary, and to make refinements on the created 3D-image.

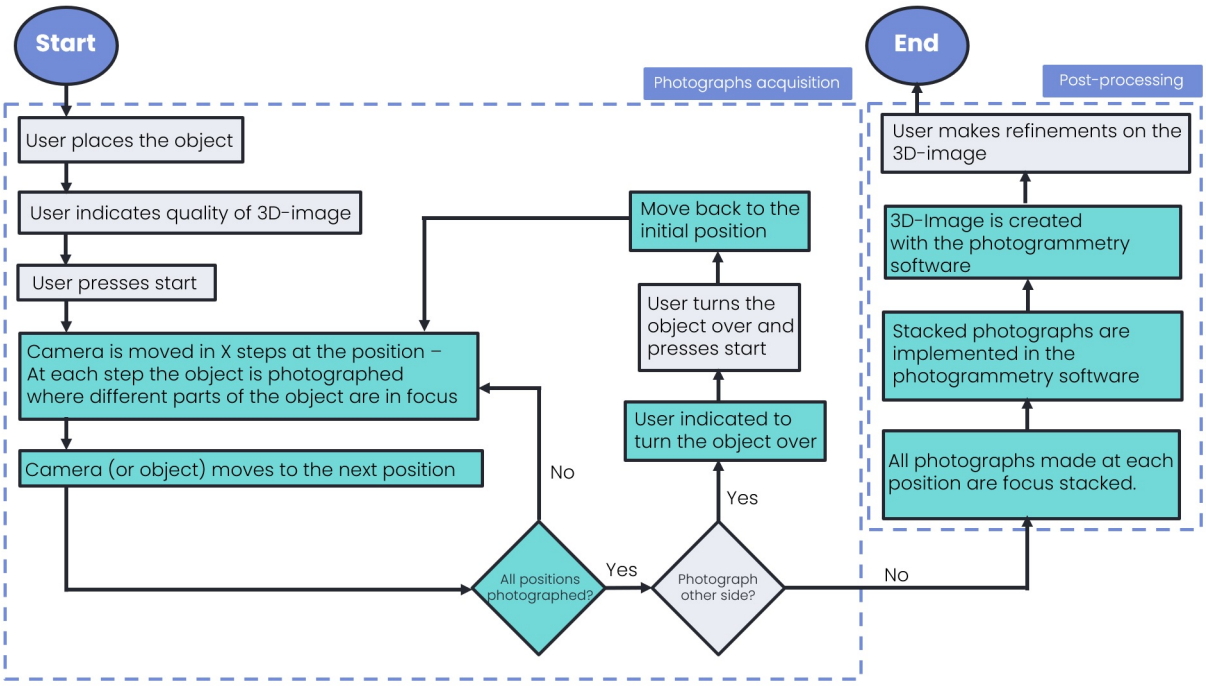

Figure 4.1: Flowchart of the workflow. The operations in gray indicate operations that the user of the system must do. The operations in blue indicate operations that are done by the system itself. The tasks that the system user must do in photographs acquisition will only last a few seconds, and the task in the post-processing maximum of 10 minutes. The photographs acquisition done by the system will last the most time in this part of the process, depending on the desired quality of the 3D-image. In this part of the process, the user does not have to be present. The user can return when the system is done to indicate whether another set of photographs must be made. Then the made photographs are post-processed. The time duration of this will depend on the number of photographs and the desired quality of the 3D-image. The system user only has to be present at the end to check the 3D-image and make refinements.

4.2. Requirements

After determining what the workflow will be for the system, the requirements for the system are determined. The requirements for the system are the following:

- **Object size requirement:** The system will be designed for objects that have a length and width between $2cm$ and $5cm$.
  - The system will be designed to make 3D-images of small archaeological objects.
- **Object handling requirement:** The object itself should not be tilted to prevent damaging the object.
  - Mounting the object can damage it. Also, by moving the object in tilted positions, the risk exists that it will be damaged. Therefore, the object movement will be limited to rotation on a horizontal plane to avoid damaging the object.
  - To photograph the object at different tilted angles, the camera should move to the desired position to prevent risking damaging the object.
- **Photographing requirement:** Take photographs 360° around the object and at tilted positions.
  - To be able to make photograph sets with different overlap percentages.
  - To capture the details of the object's top side and create a complete 3D-image of the object.

- **Focus stacking requirement:** Multiple photographs at each position in steps.
  - In order to solve the small depth-of-field problem, multiple photographs at each position where different parts of the object are in focus need to be made. These photographs will be stacked together to create one full-in-focus high-resolution image of the object. The depth of field will determine the step size.
- **Stability requirement:** Camera and object follow a stable predefined movement.
  - Vibrations should be limited to avoid motion blur when making a photograph when moving to a new position. Therefore, a stable system should be designed, where the camera and lens experience little to no vibrations when the movement comes to a stop.
  - High precision and accuracy are not of the highest relevance. What truly is important is to limit the vibrations to the camera sensor, to accurately capture sharp photographs of the object where the object is partly in focus.
- **Lighting requirement:** Good lighting setup, no strong shadows on the object and strong reflections avoided.
  - To observe the object's texture details and color information, a good lighting setup is required to create high-quality photographs of the object.
- **Cost-effective requirement:** The system should be designed with cost-effective parts so that it can be affordable for cultural heritage institutions.
- **Environmental requirement:** The system will be placed on a table. The environment should not cause external disturbances that will cause the table on which the system is placed to vibrate. If the system's environment causes vibrations, motion blur will occur, which is undesired.
- **Ease of use requirement:** Archaeologists with no previous experience with photogrammetry should be able to use the device.
  - Level of automation: only a few simple manual steps should be required because the system works automated chiefly.
  - Design for assembly: the system can be built by the user with a simple toolkit.
  - Compact: to maintain a small volume, a compact system will be desired so that the system can easily be integrated into the workspace of an archaeologist.
- **Speed:** Acquisition of the photographs for one object should be done within 60 minutes.

4.3. Specifications

The current automated systems that create high-quality 3D-images of small archaeological artifacts are very expensive. Prices can range from 10K to 50K [6]. Most cultural heritage institutions run on a small budget and cannot afford such systems. Cheaper alternative systems exist that only utilize photogrammetry as a technique to create 3D-images of objects. The 3D-images created by these systems lack detail in the object's texture due to a reduced depth of field [16]. Therefore, there is a need for a cost-effective system that can create high-quality 3D images of small archaeological objects.

This project aims to design a cost-effective photogrammetric 3D-imaging system for small archaeological artifacts. This design will optimize the depth of field to create high-quality 3D-images. This design would then create higher-quality 3D-images compared to other cost-effective solutions. This design can then be further developed, and it can then be used by archaeologists and researchers all around the globe. They will be able to use the system without further required knowledge about photogrammetry.

4.4. Conceptual system overview

The complete system can be divided into the following sub-systems: the photographing sub-system, the positioning sub-system, and the lighting sub-system. The components and functions that belong to these sub-systems are indicated to create a conceptual system overview. In Figure 4.2 the conceptual overview is depicted.

For the photographing sub-system, the following components are needed: a camera and a lens. The type of camera selected will determine how the camera can be controlled and the quality of the camera sensor. The lens will determine the field of view and the depth of field.

The following components and functions describe the positioning sub-system: the way focus stacking is going to be achieved, the actuators that are going to be used to drive the mechanisms, the guiding mechanism to guide the movable parts, the tilt mechanism that is going to be used to tilt the camera, the object rotation mechanism, the microcontroller that is going to be used, and the control method that is going to be used to position the movable parts.

The following components and functions define the lighting sub-system: the type of light source that is going to be used, the location of the light source with respect to the object and the camera, the uniformity of the light (meaning if direct light or diffused light is going to be used), and the background of the object.

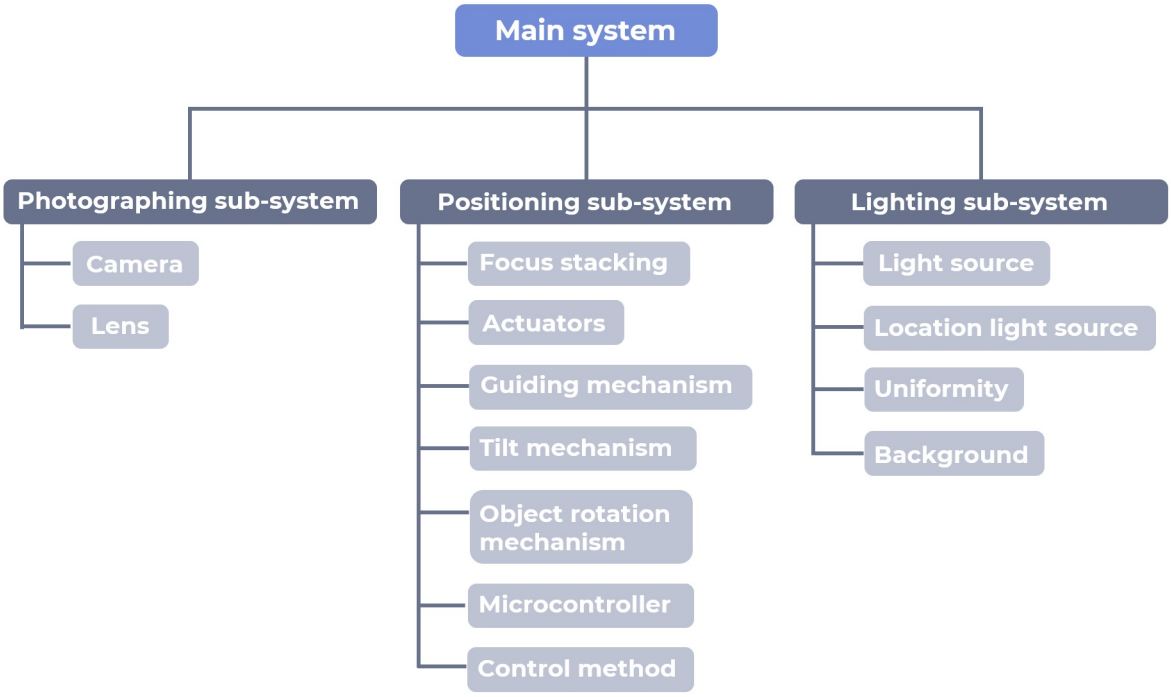

Figure 4.2: Conceptual system overview. For each sub-system, the relevant components and functions have been listed.

4.5. Challenges

There are a couple of challenges imposed when designing a photogrammetric 3D-imaging system that has been described in the previous chapters. These challenges will be addressed when making system choices and designing the system. These challenges are the following:

Designing a stable and fast system
To design a fast photogrammetric 3D-imaging system, the system should stabilize fast enough after being moved. The faster the system stabilizes when it comes to a standstill after giving it an impulse, the faster the system will be. The photograph can then be taken as fast as possible without motion blur, and the camera or object can be moved to the next position. Ideally, the photograph would be taken immediately after the camera or object comes to a standstill. What also makes designing this system challenging is that the object has to be minimally moved.

Good lighting setup
Designing a good lighting setup is challenging because the lighting setup has to be integrated with the mechanism that positions the camera and the object. Lighting orientation to prevent unwanted strong shadows and reflections is an important aspect. It is essential to consider where the light will be placed and how it will be oriented with respect to the camera and the object. Also, lighting for different shapes that objects can have has to be acknowledged.

Integration of all the components
The integration of all the components and sub-systems is a challenge in itself. The photographing, positioning, and lighting sub-system have to be integrated to form the complete system. Considerations on how the actuators and camera will be controlled are part of this challenge.

Cost-effective
To make a photogrammetric 3D-imaging system that will be cost-effective for it to be affordable for heritage institutions comes with a challenge. The components selection involved for each sub-system requires research on the available components on the marketplace that are cost-effective. One example of this is the camera and lens combination selection that will be used for the system.

Optimization
Another challenge is the optimization of the photogrammetric 3D-imaging system. This includes optimizing the actual system used to acquire the photographs of the object and the optimization of the resulting 3D-image. Different factors influence the quality of the resulting 3D-image. These factors are, among other things, overlap percentage, use of markers, and the trajectories used for making photographs. The named factors should be studied, and the resulting 3D-images should be assessed. To find an optimum regarding the quality of the 3D-image and the time needed to acquire it. This is another challenge, to quantitatively assess the quality of the 3D-images to make sound conclusions about an optimum.

Focus stacking
One more challenge is the one involved with integrating focus stacking in a photogrammetric 3D-imaging system. The aspects that have to be considered are focus stacking for different object sizes and focus stacking for complex geometries. The number of photographs per position to create a focus stacked image should be minimized. By doing so, the system will be faster because fewer photographs need to be taken. Also, the post-processing part of the workflow will be faster because fewer photographs have to be processed, and only the necessary photographs will be used.

4.6. Components for the system

One of the requirements of this project is to achieve a cost-effective design with widely available components. Therefore, for this project, components will be used that are cost-effective and widely available. Components that meet these requirements are 3D-printed parts, laser cut parts, components used in 3D printers and printers, generic electrical components, and other off-the-shelf components.

4.7. Concept generation

A concept will be generated with the following approach. For each of the functions and components of the sub-systems, potential solutions will be conceived. In Figure 4.3 a morphological table is shown where the possible solutions that have been conceived for each component and function can be seen. The potential solutions will be compared, and system choices will be made while considering the system requirements to generate a concept. The concept will be generated by choosing the best solution for each component and function per sub-system. The concept will be generated while taking into account the other sub-systems and necessary components. By selecting a solution for each component and function, the concept is composed of individual component and function choices. These individual component choices will be combined well to develop a concept. The system choices and selection of the possible solutions for each of the components and functions will be substantiated in the concept selection subchapter 4.8, and the final concept will be determined in this subchapter. This final concept will be further developed in Chapter 5 to create a detailed design of the system.

Main system	Solutions			
Photographing sub-system				
Camera	Raspberry Pi HQ Camera	Compact camera	USB camera	Mobile camera
Lens	Prime lens	Zoom lens		
Positioning sub-system				
Focus stacking	Mechanically changing focus	Moving the camera with fixed focus		
Actuators	Stepper motor	Servo motor	Linear motor	
Guiding mechanism	Belt-driven mechanism	Screw-driven mechanism	Chain-driven mechanism	
Tilt mechanism	Slider mechanism	Direct drive torque mechanism	Vertical actuation	
Object rotation mechanism	Turntable			
Microcontroller	Arduino Uno R3	Raspberry Pi 4B	BeagleBone Black	
Control method	Feedforward	Feedback		
Lighting sub-system				
Light source	Incandescent bulbs	Halogen bulbs	LED	CFL
Location light source	Moving with respect to the object	Fixed with respect to the object		
Uniformity	Pointing directly at the object	Diffused lighting setup		
Background	White	Black		

Figure 4.3: Morphological table that is used to generate the concept that will be further developed.

4.8. Concept selection

In this subchapter, the choices for the components and functions arranged per subsystem will be substantiated. Afterward, the complete concept is created and will be further developed in Chapter 5 by doing dimensional calculations to create a detailed design of the concept.

4.8.1. Photographing subsystem

Camera

Different affordable cameras have been considered and compared. Compact cameras, USB cameras, Raspberry Pi HQ Camera, and using mobile cameras have been considered. Raspberry Pi HQ Camera has been chosen as the camera to use for this project. The reasons are the following.

- **Compatibility:** The Raspberry Pi HQ Camera can easily be integrated into the design and is widely available. It has several mounting options. Choosing the camera for the system avoids compatibility issues than when for example, choosing for a mobile camera. Then it must be taken into account that there are different types of mobile phones and can result in a complex design. The Raspberry Pi HQ Camera is controlled with a Raspberry Pi microcontroller, which can also be used to control the actuators.

- **Price and quality:** The price of the camera is €43, which is a cost-effective component. The camera sensor has 12.3 megapixels which is a high resolution compared to the cameras that are available.
- **Lens options:** The camera has diverse lens mounting options. C-mount and CS-mount lenses are supported.
- **Lightweight:** The camera is lightweight, weighing 10 grams. By having a lightweight camera, less powerful actuators will be needed.

Lens

There are two types of lenses that have to be considered: a prime lens and a zoom lens. A prime lens is a lens with a fixed focal length. A zoom lens can change the focal length, thus controlling which part of the object is in focus when photographed. The zoom lens can also be used with a fixed focal length. When using a prime lens or a zoom lens with a fixed focal length, the camera has to be moved to move the focus plane through the object and photograph all the parts of the object in focus separately. Since most of the lenses that Raspberry provides are zoom lenses, a zoom lens will be used. Also, a zoom lens provides more flexibility to configure the system. In Chapter 5, it will be discussed which zoom lens will be used.

4.8.2. Positioning subsystem

Focus stacking

The focus stacking function of the system can be achieved in two ways. One way is by mechanically changing the focal length of the zoom lens, and another way is by moving the camera with a fixed focus. It has been chosen to achieve focus stacking by moving the camera with a fixed focus. The reason for this is because it is more stable than mechanically changing the focal length of the zoom lens and also results in a less complex design. Mechanically changing the focal length may result in instability because of the possible play in the zoom lens.

Actuators

Three actuators will be needed for this system: one to rotate the object, one to move the camera, and one to tilt the camera. A variety of electric actuators have been considered for this system. The electrical actuators that have been considered are stepper motors, servo motors, and linear motors. For this system, it has been chosen to use a stepper motor. It provides stable movement and accurate motion that can be used for the movement of the camera, the tilting mechanism, and the turntable. The advantage of using a stepper motor is that it is open-loop, so there is no need for a sensor, resulting in a cost-effective solution for the system. The reason why linear motors are not chosen is that they require a sensor system and feedback control. Linear motors would result in a more complex and expensive design and are not necessary for this project. Stepper motors are chosen and not servo motors because stepper motors are more cost-effective and more compact. Servo motors can operate at higher speeds and higher accelerations. However, as a result, a servo motor can be up to an order of magnitude more expensive than a comparable stepper motor [15].

Guiding mechanism

Three guiding mechanisms have been considered: belt-driven, screw-driven, and chain-driven. The chosen guiding mechanism is screw-driven because it is cost-effective, lightweight, quick response, smooth, and self-locking with the right pitch and diameter ratio [17]. By having a self-locking guiding mechanism, a more stable system is designed. Screw-driven guiding mechanisms work in the following way. By having a lead screw connected to a mover with a lead screw nut that is fixed to the mover, and another guiding axis that constrains the rotation of the mover, the mover, is moved linearly when an actuator rotates the lead screw. The rotary motion of the actuator translates into a linear motion. The disadvantage of a leadscrew mechanism is that it has limited speed abilities compared to, for example,

a belt-driven mechanism. A chain-driven mechanism is not chosen because it will be heavier than a leadscrew and belt-driven mechanism, requiring more powerful actuators. A leadscrew guiding mechanism is desired because the camera is also going to be in tilted positions. The self-locking feature of this guiding mechanism is useful for tilted positions and creates stability. Otherwise, a constant torque would be needed to hold the camera in place. If this holding torque is not completely constant the whole time, it will result in instability and motion blur. Self-locking also makes the system less subjective to external disturbances that can cause motion blur.

Tilt mechanism

Three types of tilting mechanisms were considered for the tilting mechanism: slider mechanism that uses a lever, direct-drive torque mechanism that directly tilts the camera, and a vertical actuation concept where the camera is tilted. The slider mechanism that uses a lever is the tilt mechanism that is chosen for the system. The direct-drive torque mechanism is not chosen because a more powerful actuator will be needed, or a gear reduction system would have to be designed with a less powerful actuator. The direct-drive torque mechanism is also prone to instability if constant torque cannot be maintained. The vertical actuation mechanism is not chosen because it will result in a complex design with a sliding component on the mover where the camera is supported to achieve tilt by vertical actuation. The slider mechanism will be easier to implement, and less powerful actuators will be needed. The design of the tilt mechanism is discussed in Chapter 5.

Object rotation mechanism

The only motion that the object will experience is planar rotation to prevent potentially damaging the object. A simple turntable with a stepper motor will be built and used to rotate the object. As the object that is going to be rotated is lightweight, there is no need for a gear reduction mechanism to increase the torque. Therefore, the turntable can be directly connected to the actuator, resulting in a straightforward design.

Microcontroller

A variety of microcontrollers have been considered to control the actuators that will be used in the design. The microcontrollers that were considered were: the Arduino Uno R3, The Raspberry Pi 4B, and the Beaglebone Black. The Raspberry Pi 4B microcontroller has been selected because it can control both the Raspberry Pi HQ camera and the actuators.

Control method

The type of actuator that has been chosen to be used for the system is a stepper motor. The stepper motor is accurate enough and provides precise movements for the three movements that the system has to do: the rotation of the object, the movement of the camera, and the movement of the tilting mechanism. The stepper motor operates in an open-loop, so there is no need for a sensor. Vibrations caused by the motion when moving to the next position can cause motion blur to the photograph when taking it too rapidly after moving to the next step. To minimize vibrations, the lens and camera should be stiffly connected to the part that is being moved in each step. The system should be stiff and have enough mechanical damping to minimize vibrations. By minimizing the vibrations with each movement to the next position, the time needed to wait between taking photographs is reduced. And therefore, the photographs acquisition time is also reduced. If the loss of steps with the stepper is too great due to the friction the stepper motors experience, feed-forward could be implemented if the system behavior is known and repeatable.

4.8.3. Lighting subsystem

Light source

Different types of light sources have been considered: incandescent bulbs, halogen bulbs, LEDs (Light

Emittent Diode), and CFL's (Compact Fluorescent Lamp). LED has been chosen because LED strips can be easily integrated into the design. LEDs can also provide high intensity/brightness. LEDs also offer directional lighting, which can be used for the lighting setup.

Location light source

To avoid different shadowing, glare, and reflections in each photograph, the location of the light source will be fixed with respect to the object. By doing it this way, the object is photographed with the same lighting at each position. By not doing this, a less accurate representation of the object will be created with the 3D-image. It will be less accurate because the shadows, glares, and reflections will be different at each position in each photograph, resulting in an unnatural 3D-image of the object.

Uniformity

In order to avoid strong shadows and reflections, direct light will be avoided. Uniform lighting with a diffused lighting setup will be used. When the object is illuminated directly by a point-shaped light source, many surfaces that are glossy to an extent will show bright reflections. To avoid this, a diffused lighting setup will be used. As LEDs are a collection of point sources, this will cause light spots/brighter patches on the object, which is not desired. Therefore, it is desired to use diffused light, creating a more even illumination. The only downside when using diffused light is that the intensity is often reduced. Therefore the amount of LED lights and intensity should be chosen accordingly.

Background

For the background of the object, a white and black background has been considered. A white background has been selected to be able to create a diffused lighting setup. White reflects light, and a diffused lighting setup can be created by pointing the light source at a white background and not directly at the object. The white surface will reflect the light onto the object to illuminate it.

4.8.4. Final concept

Main system	Solutions			
Photographing sub-system				
Camera	Raspberry Pi HQ Camera	Compact camera	USB camera	Mobile camera
Lens	Prime lens	Zoom lens		
Positioning sub-system				
Focus stacking	Mechanically changing focus	Moving the camera with fixed focus		
Actuators	Stepper motor	Servo motor	Linear motor	
Guiding mechanism	Belt-driven mechanism	Screw-driven mechanism	Chain-driven mechanism	
Tilt mechanism	Slider mechanism	Direct drive torque mechanism	Vertical actuation	
Object rotation mechanism	Turntable			
Microcontroller	Arduino Uno R3	Raspberry Pi 4B	BeagleBone Black	
Control method	Feedforward	Feedback		
Lighting sub-system				
Light source	Incandescent bulbs	Halogen bulbs	LED	CFL
Location light source	Moving with respect to the object	Fixed with respect to the object		
Uniformity	Pointing directly at the object	Diffused lighting setup		
Background	White	Black		

Figure 4.4: In this Figure, the final concept is shown that will be further developed. In blue, the chosen solution for each of the functions and components of the sub-systems are shown.

In Figure 4.4, the final concept is shown that has been discussed in the previous subchapters. In Chapter 5, the detailed design of the system is presented.

5

Detailed system design

In this chapter, the detailed design of the system is discussed. This chapter includes the lens calculations and lens choice, the tilt mechanism design, the guiding mechanism design, the lighting setup design and turntable design, the integration of all system components and complete design, the required torque calculations, the stepper motor calculations and considerations, the stress analysis of the critical components, the stability considerations, and finally the cost overview.

5.1. Lens calculation and lens choice

To choose whether what lens will be used with the Raspberry Pi HQ camera, calculations must be done. It must be calculated what the lens's focal length should be to obtain the desired field of view, where the object almost completely utilizes the area of the camera sensor. The system will be designed for objects between 2 and 5 cm. Therefore, the lens will be chosen so that the biggest possible object fits into the field of view.

The focal length and field of view are related in the following way. The field of view is directly related to the focal length of a lens. When the focal length is shorter, the field of view is wider with greater area captured, and when the focal length is longer, the field of view is narrower where objects seem to appear larger.

The Raspberry Pi HQ camera has a crop factor of 5.5. The crop factor is the ratio of the dimensions of a camera's imaging area compared to a reference format. The crop factor of a camera sensor is determined by dividing its diagonal dimension by the diagonal dimension of a "full-frame" sensor, 43.3mm. The Raspberry Pi HQ camera has a sensor size of 6.287mm x 4.712mm. By using the Pythagorean theorem, it can be determined that the diagonal size of this sensor is 7.85mm. Now, taking 43.3mm and dividing it by the diagonal size of this sensor, a crop factor of 5.5 is found [2]. To calculate the effective focal length of the lens, the focal length of the lens has to be multiplied by the crop factor of 5.5 when the lens is used with the Raspberry Pi HQ Camera [22].

To obtain the equation that calculates the field of view, the following equations need to be worked out. First, the lens equation is written down in Equation 5.1, where f is the focal length, v is the object distance, and b is the image distance. See Figure 5.1.

$$\frac{1}{f} = \frac{1}{v} + \frac{1}{b} \tag{5.1}$$

The equation for the magnification is shown in Equation 5.2, where y' is the image height and y is the object height.

$$M = \frac{y'}{y} = \frac{b}{v} \tag{5.2}$$

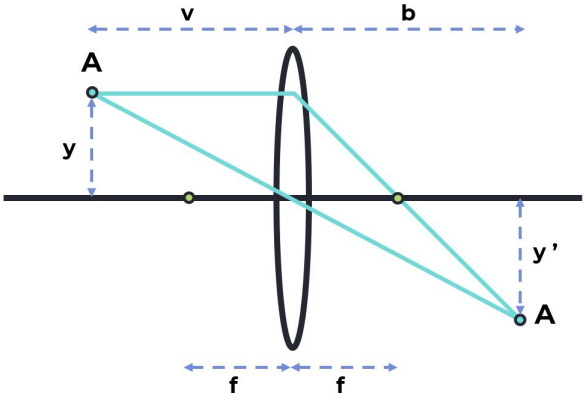

Figure 5.1: Geometric optical presentation of the lens equation.

By rewriting the equation for the maginification, Equation 5.3 is gathered.

$$b = \frac{vy'}{y} \tag{5.3}$$

By rewriting the lens equation, Equation 5.4 is obtained.

$$\frac{1}{f} = \frac{1}{v} + \frac{y}{vy'} \tag{5.4}$$

And finally, by rewriting Equation 5.4, Equation 5.5 can be obtained. With this equation the object height y, which is the field of view in the y-direction, can be calculated.

$$y = (\frac{v}{f} - 1)y' \tag{5.5}$$

The same equation can be written for the field of view in the x-direction by interchanging the variables. This is shown in Equation 5.6.

$$x = (\frac{v}{f} - 1)x' \tag{5.6}$$

The equations to calculate the field of view are shown in Equation 5.5 and 5.6. Where x and y are the field of view in the x- and y-direction, f is the focal length, and x' and y' are the size of the image in the x- and y-direction, which are the dimensions of the sensor. x' and y' are 6.287 mm and 4.712 respectively. The available Raspberry Pi lenses for the Raspberry Pi HQ camera have a focal length of 16mm and 6mm. The effective focal lengths of these lenses, taking into account the crop factor of the camera sensor, are 88mm and 33mm, respectively.

When filling in the equations for the field of view with an object distance of 180mm, a field of view in the x-direction and y-direction of 6.6 mm and 4.9 mm, respectively, is obtained. This is too small, so another lens should be added to the lens configuration, to obtain a field of view of at least 50 mm in the y-direction. A lens with a focal length of 3 mm that is compatible with the 16mm Raspberry Pi lens will be added to the lens configuration. The combined focal length can be calculated with Equation 5.7 [14].

$$\frac{1}{f} = \frac{1}{f_1} + \frac{1}{f_2} \tag{5.7}$$

Filling in and solving Equation 5.7 for f, where f_1 and f_2 are 16mm and 3mm, respectively, results in a combined focal length f of approximately 2.5mm. Calculating the field of view with the newly obtained focal length, where the effective focal length is now 13.8mm, results in a field of view of 76mm and 57mm in the x- and y-direction, respectively. This is the desired field of view, so the lens configuration is complete by using the Raspberry Pi 16mm lens and an additional 3mm lens.

5.2. Tilt mechanism design

As discussed in Chapter 4, the tilt mechanism design will be a slider mechanism with a lever. A schematic drawing of the designed slider mechanism to tilt the camera is shown in Figure 5.2.

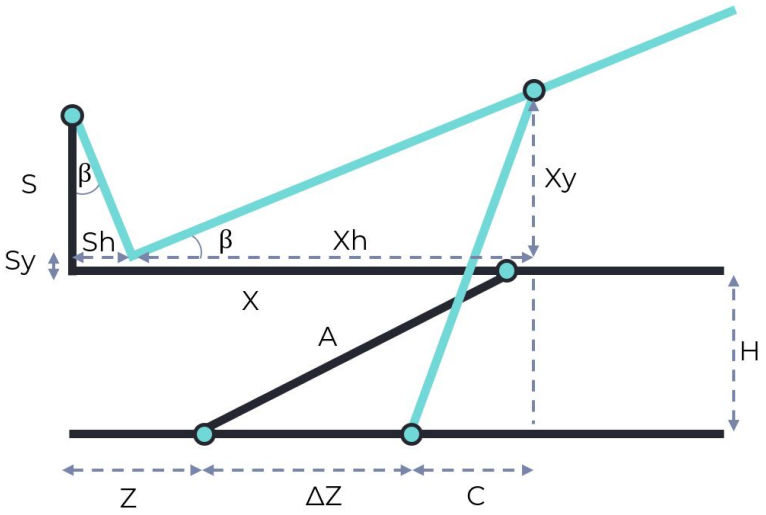

Figure 5.2: Schematic drawing of the designed slider mechanism to tilt the camera. When a displacement ΔZ is done, the camera and mechanism that moves the camera will be tilted by an angle β.

Dimensional calculation

To compute the relationship between the achieved tilt β and the displacement ΔZ to tilt the mechanism as indicated in Figure 5.2, the following trigonometric calculations were done. Firstly, the following equations for the variables Sh, Sy, Xh, and Xy are set up.

$$Sh = S \cdot sin(\beta) \tag{5.8}$$

$$Sy = S - S \cdot cos(\beta) \tag{5.9}$$

$$Xh = X \cdot cos(\beta) \tag{5.10}$$

$$Xy = X \cdot sin(\beta) \tag{5.11}$$

Then, the equation to find the variable C is the following:

$$A^2 = C^2 + (H + Sy + Xy)^2 \tag{5.12}$$

Rewriting the above equation results in:

$$C = \sqrt{A^2 - (H + Sy + Xy)^2} \tag{5.13}$$

And it is also known that:

$$Sh + Xh = Z + \Delta Z + C \tag{5.14}$$

Rewriting this results in:

$$\Delta Z = Sh + Xh - Z - C \tag{5.15}$$

With Sh, Xh, Z, and C known, the equation for ΔZ expressed in the achieved tilt β can be computed, which is shown in Equation 5.16.

$$\Delta Z = S \cdot sin(\beta) + X \cdot cos(\beta) - Z - \sqrt{A^2 - (X \cdot sin(\beta) + S - S \cdot cos(\beta) + H)^2} \tag{5.16}$$

Dimensional design considerations
To ensure that the object's field of view is maintained as much as possible in the tilted position, the tilting point of the tilt mechanism should be positioned in the middle of the turntable. By doing so, the dimensions Z, S, and H are determined by the size of the turntable and the size of the guiding mechanism used for the movement of the camera. To achieve the highest amount of tilt, H should be as small as possible. By making H as small as possible, the system will be more compact. However, making it too small while maintaining the same dimensions and connection points for the link with dimension A, will increase the reaction forces in the x-direction on the joint positioned at a distance Z, requiring a higher torque to tilt the mechanism. The higher reaction forces will also increase the stresses on the supporting joints. Increasing the distance X will also increase the achievable tilt, but this is undesired because it would make the system less compact. Keeping the dimension S as small as possible also increases the achievable tilt, but this dimension is determined by the size of the guiding mechanism for the camera. The relationship between the displacement ΔZ and the achieved tilt β is nonlinear. This is shown in Figure 5.3. It can be seen that most of the tilt is achieved in the first part of moving the tilt mechanism. The tilt increase in the last part of the movement of the tilt mechanism is negligible. Therefore, only the displacement will be done to tilt the mechanism where most of the tilt is achieved.

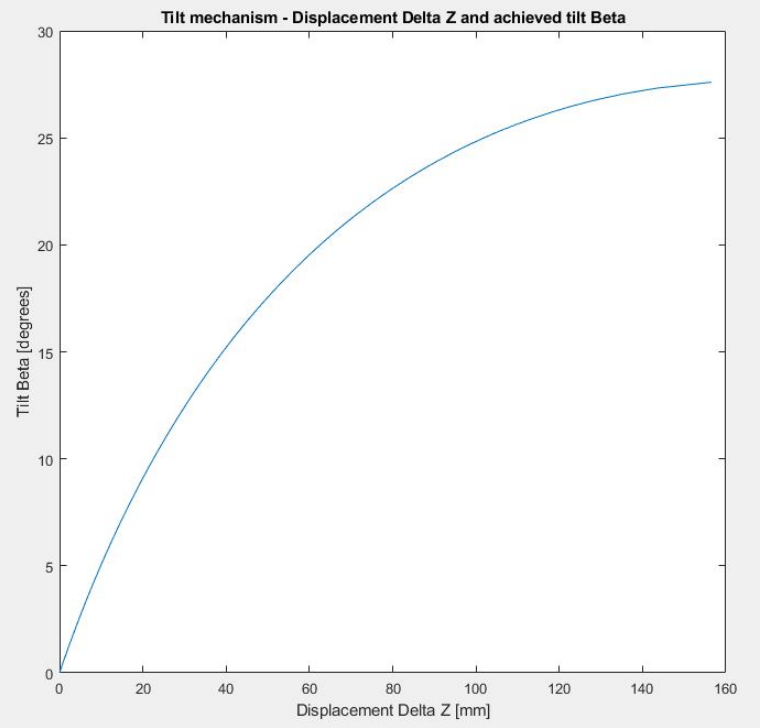

Figure 5.3: Displacement ΔZ versus achieved tilt β.

5.3. Guiding mechanism design

The guiding mechanism that is discussed in this subchapter will be used for two movements. It will be used to move the camera, and secondly, it will be used to move the tilt mechanism that is holding the camera and the guiding mechanism of the camera. The system choice has been made to use a leadscrew as the guiding mechanism in the conceptual system design. By using a leadscrew, that is fixed at both ends of the leadscrew axis and mounted with a leadscrew nut to the mover on which the camera is supporting, four of the six degrees of freedom are constrained. The degrees of freedom are shown in Figure 5.4. The Zt, Zr, Yt, and Yr degrees of freedom are constrained by the leadscrew axis alone.

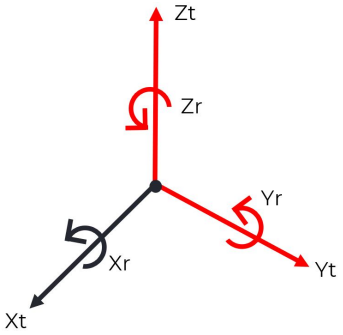

Figure 5.4: Degrees of freedom shown in black after using a leadscrew as a guiding mechanism. The red degrees of freedom are constrained.

The only desired degree of freedom is the translation in the x-direction, Xt, as shown in Figure 5.4. To accomplish this, the rotation about the x-axis, Xr, should be constrained. This can be accomplished by adding another guiding axis parallel to the leadscrew axis. This guiding axis will be made out of steel. Linear roller bearings will be clamped in the 3D-printed mover on which the camera and lens are fixed to allow it to move along the guiding axis. To increase the stiffness of the design, two guiding axes will be used to guide the mover instead of one. This will make the design overconstrained, but it will be done with the purpose of creating a stable system. Figure 5.5 shows the guiding mechanism design. In total, four linear roller bearings will be used to support the mover onto the guiding axes. Also, by having a symmetrical design with two guiding axes, the torque exerted on the mover will be equally distributed over the two guiding axes. This creates more stability. If only one guiding axis were used, this would not be the case. To ensure that the camera and lens are stiffly connected to the mover, a lens clamp is used.

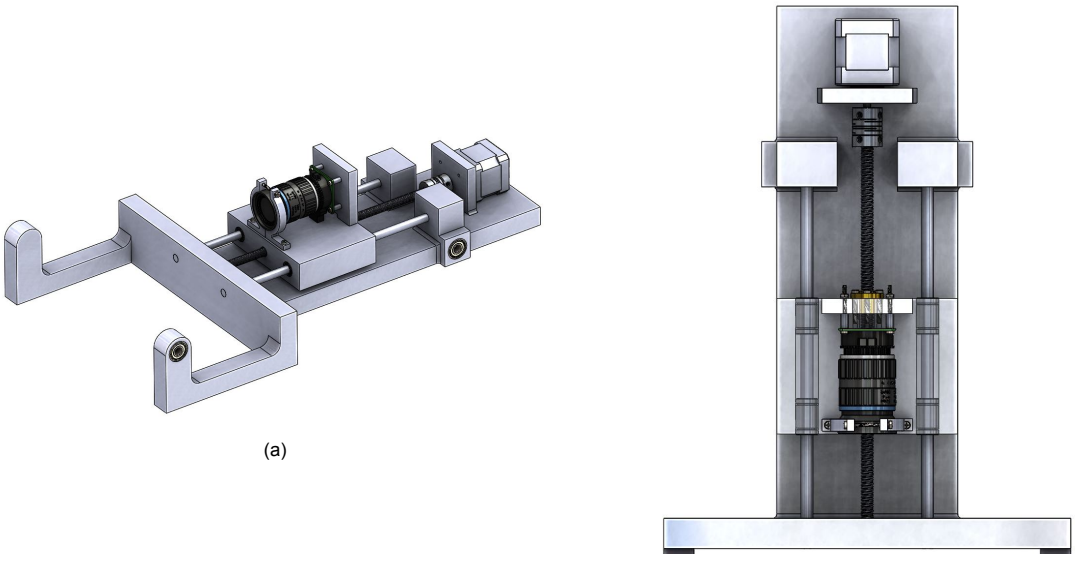

(a) (b)

Figure 5.5: Guiding mechanism for the camera mover. **(a)** Side view. **(b)** Top view where the mover is transparent and the linear roller bearings are visible.

By having two steel guiding axes with four linear roller bearings, resulting in an overconstrained guiding mechanism, the friction that is needed to be overcome to make the mover move when the leadscrew is actuated will increase. Not only that, the small inaccuracies that occur when aligning the four linear roller bearings, a leadscrew, and the two steel guiding axes, will cause additional friction when actuating the mover. Perfectly lining up the three axes is difficult. Due to the small inaccuracies of the components, the axes will not be perfectly aligned. However, this effect is used as an advantage. The additional friction created will function as mechanical damping, reducing the vibrations when the camera is moved.

By doing so, a more stable system is created that can take the next photograph faster after moving to the next position.

The guiding mechanism for the tilt mechanism mover will have a similar design. However, since the 3D-printed part can be smaller because there is no camera supporting on it, it will only have two linear roller bearings. The stability of this part is essential because instability will result in motion blur. This is because it is indirectly connected to the camera. As mentioned before, the leadscrew will be self-locking, and therefore the mover to tilt the mechanism will have little to no play and will be stable.

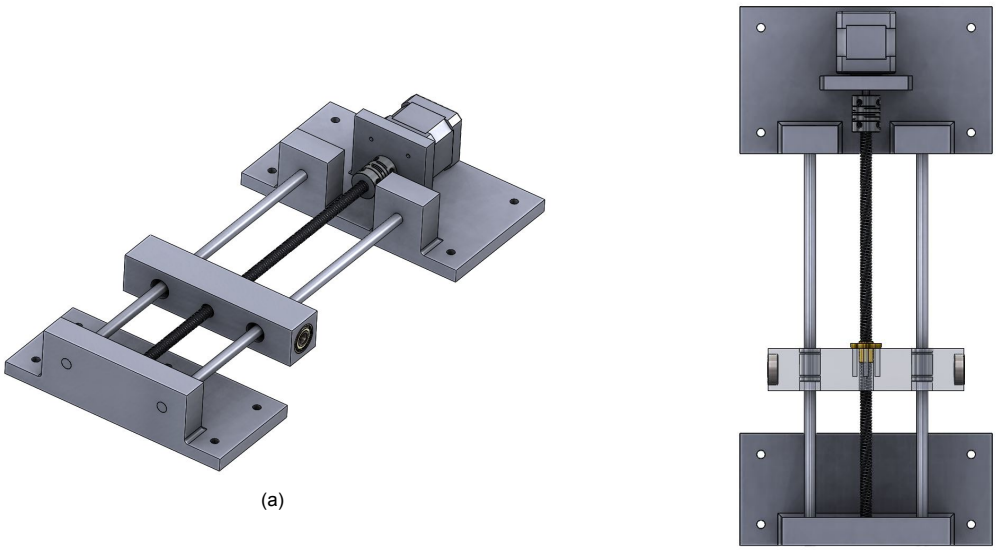

(a) (b)

Figure 5.6: Guiding mechanism for the tilt mechanism mover. **(a)** Side view. **(b)** Top view where the mover is transparent and the linear roller bearings are visible.

To achieve a self-locking leadscrew, the friction angle θ must be greater than the lead angle λ [30]. In Figure 5.7 the lead angle is depicted. In Equation 5.17 and 5.18 it is shown how θ and λ are calculated.

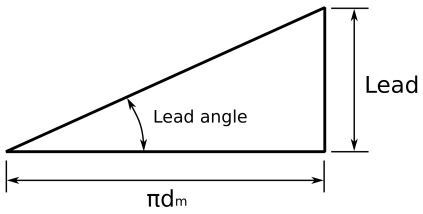

Figure 5.7: Schematic drawing to calculate the lead angle of a leadscrew, where d_m is the mean diameter of the leadscrew.

$$\theta = tan^{-1}(\mu_s) \tag{5.17}$$

$$\lambda = tan^{-1}(\frac{Lead}{\pi \cdot d_m}) \tag{5.18}$$

The friction coefficient μ_s for a leadscrew and leadscrew nut is 0.2. By filling in the equations for a leadscrew with a diameter of 8mm and a lead of 2mm, it is calculated that it is self-locking. Therefore, a leadscrew with these dimensions is used. The leadscrew will be connected with a flexible coupling to the stepper motor, as can be seen in Figure 5.5 and 5.6. The purpose of a flexible coupling is to

transmit the torque from the stepper motor to the leadscrew while accepting at the same time a small amount of misalignment.

5.4. Lighting setup design and turntable design

Lighting setup design

The light source that will be used will be LED. A light-emitting diode (LED) is a semiconductor light source that emits light when current flows through it. Electrons in the semiconductor recombine with electron holes, releasing energy in the form of photons. The color of the light (corresponding to the energy of the photons) is determined by the energy required for electrons to cross the band gap of the semiconductor. White light is obtained by using multiple semiconductors or a layer of light-emitting phosphor on the semiconductor device [29].

An important quality indicator of LED is the Color Rendering Index (CRI). This index is a quantitative measure of the ability of a light source to reveal the colors of various objects faithfully in comparison with an ideal or natural light source. Therefore a LED strip with a high CRI is desirable to accurately capture the color information of the object's texture when taking a photograph. In Figure 5.8, this is clarified with an illustration of the spectrum. The CRI value is a value between 0 and 100. As the CRI becomes higher and comes near 100, the more it will resemble the desired spectrum of daylight. For this project, LED strips with 90 CRI with a color temperature of 4000K will be used. 4000K Color temperature is chosen because it is a natural clear white color, which will result in a natural representation of the object in the taken photograph.

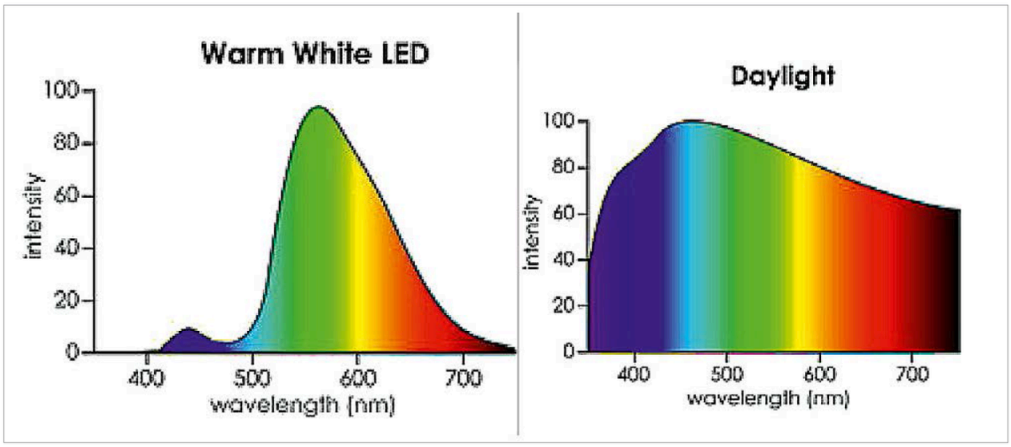

Figure 5.8: Warm white LED spectrum vs daylight spectrum [12].

As discussed in Chapter 4, the lighting setup will be a diffused lighting setup. This is because direct light onto the object will cause strong shadows, reflections, and glares. By using a diffused lighting setup, these effects are avoided. Another reason why diffused light is desired to create a more even illumination is that LED is a collection of point sources. This will cause bright spots on the object which is not desired. The only downside when using diffused light is that the intensity is often reduced. Therefore, there should be a sufficient amount of LED lights to have enough light intensity.

To achieve a diffused lighting setup, a hemispherical light dome is designed. This design is inspired by a setup that uses a similar lighting setup [23]. This light dome will be placed around the turntable. In Figure 5.9, the designed light dome can be seen. Inside the light dome, the LED strips will be placed pointing upwards on the outer circumference of the light dome. By doing so, the light is reflected from the upper white surface of the light dome onto the object, which creates diffused light. The illumination of the object is indirect and nearly homogeneous. A wall has been placed into the light dome between the object and the LED strips to prevent direct illumination of the object. A slot is made in the light dome to make photographs of the object. To not interfere with the lighting setup for the object, not create unwanted shadows, and maintain consistent lighting, the light inside the dome has to be brighter than

the light outside the dome. In Chapter 4, the system choice was made that the lighting has to be fixed with respect to the object. This lighting setup does not comply with this because of the slot that the light dome has, but the light is divided homogeneously enough to make the assumption that it resembles a lighting setup where the light is fixed with respect to the object.

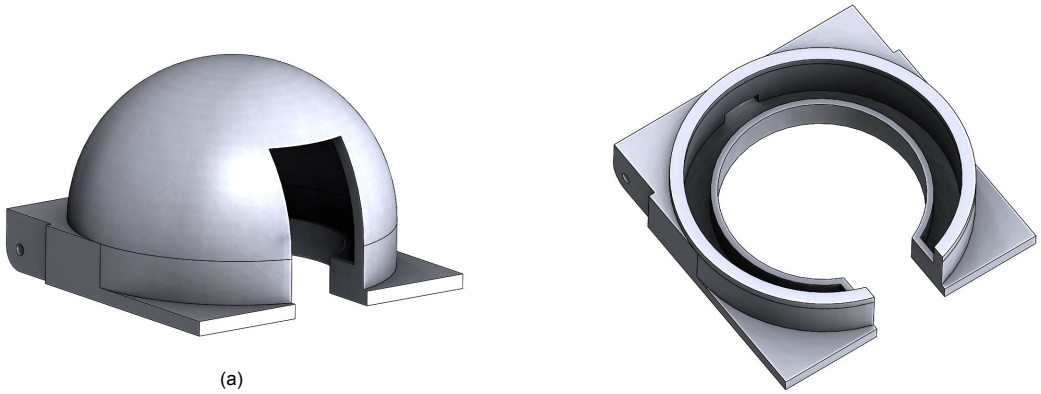

(a) (b)

Figure 5.9: The designed light dome. **(a)** Complete view. **(b)** Cross-sectional view where it can be seen where the LED strips will be placed.

Turntable design

For the turntable, a simple design was made. This design is shown in Figure 5.10. Because the objects are going to be lightweight, there is no need for a gear reduction system to increase the torque of the stepper motor. The 3D-printed turntable is directly mounted to the stepper motor axis with bolts. A form-fitting design will be used to fix the stepper motor and turntable to the base. This is depicted in Figure 5.10. The form-fitting design constrains five degrees of freedom of the turntable. The only degree of freedom left is the translation along the length of the base. This degree of freedom is needed to be able to place the stepper motor together with the turntable. The configuration will not move up along the length of the base when the stepper motor is actuated because the torque that will be used to rotate the objects will be very small. Also, the configuration is held in its place by its weight, where the stepper motor contributes to most of the weight.

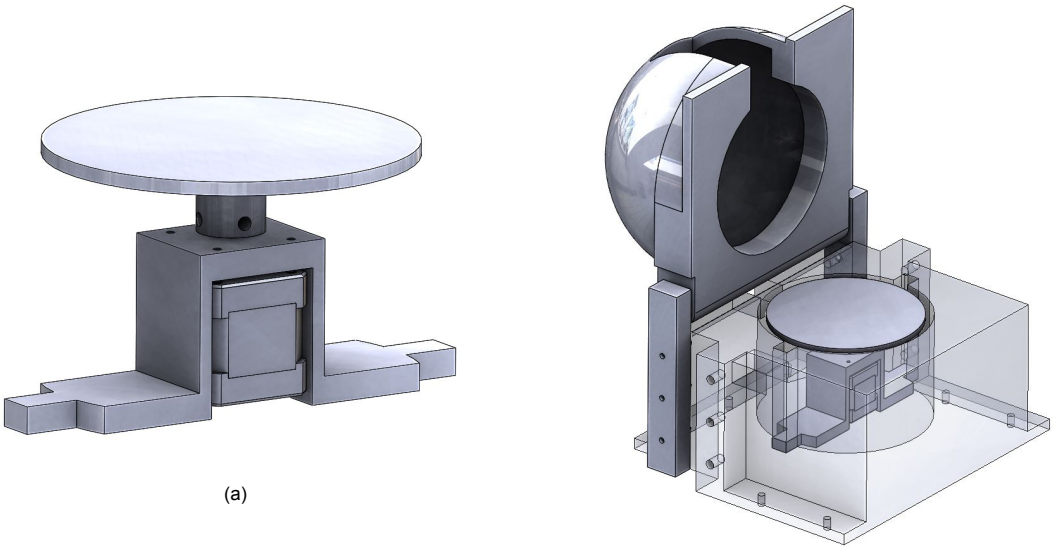

(a) (b)

Figure 5.10: The designed turntable. **(a)** 3D-printed turntable mounted to stepper motor. **(b)** Turntable implementation in the base.

5.5. Integration of all system components and complete design

In Figure 5.11, 5.12, and 5.13, the complete designed system can be seen in different positions from different views. The wooden base plate on which the system is supporting has a width of 0.63m and 0.4m. All parts are 3D-printed, except for the base plate, leadscrews, steel axes, and other obvious parts that are not 3D-printed. Two connecting links are used to connect the upper part of the tilt mechanism with the bottom part of the tilt mechanism. The stiffness of the connecting links is reinforced by using a cross-linkage to minimize possible vibrations. At the joints, steel pins with ball bearings are used to allow for rotational motion. The steel pins are glued into the 3D-printed parts. Metallic inserts are used to fasten the bolts that are used in the system. By using metallic inserts, the system can easily be disassembled. The dimensions of the tilt mechanism have been designed to achieve 30 degrees tilt. 30 Degrees tilt is sufficient to photograph the object at an angle most of the time. If the tilt is insufficient, the object can be turned around, and another set of photographs can be taken.

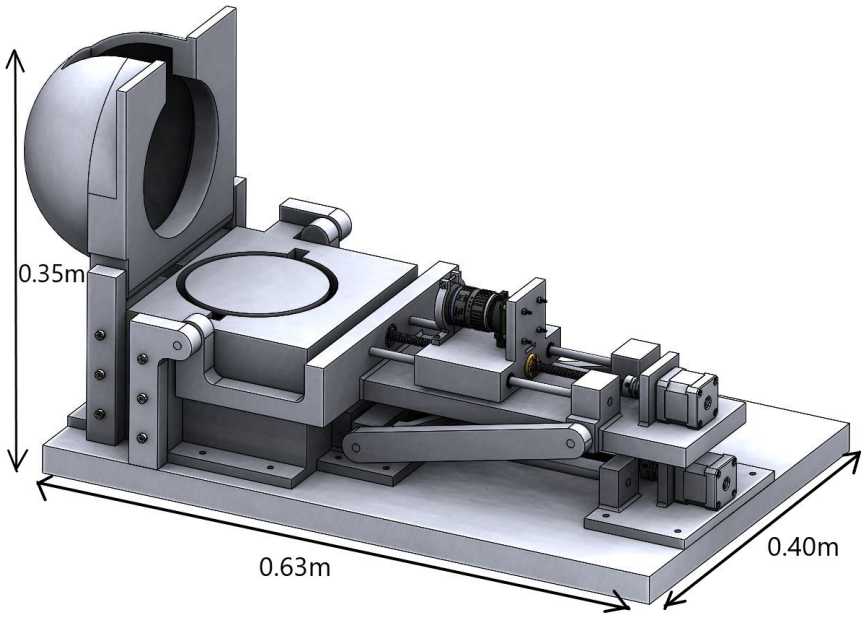

Figure 5.11: Complete system.

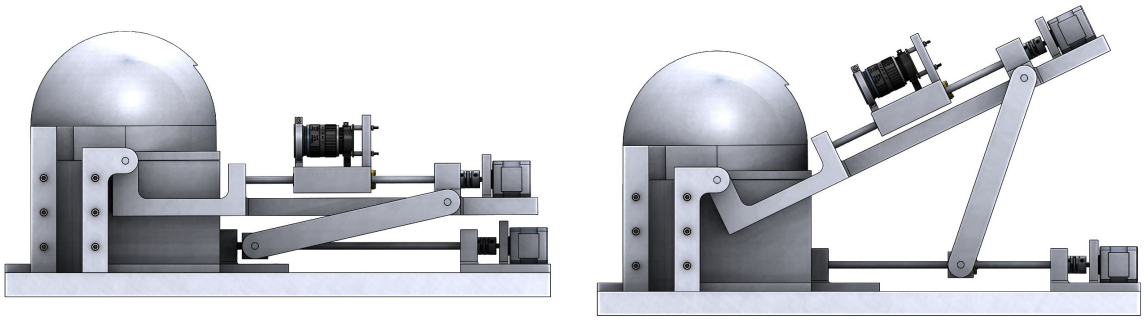

(a)

(b)

Figure 5.12: Complete system. **(a)** Side-view. **(b)** Side-view in the tilted position.

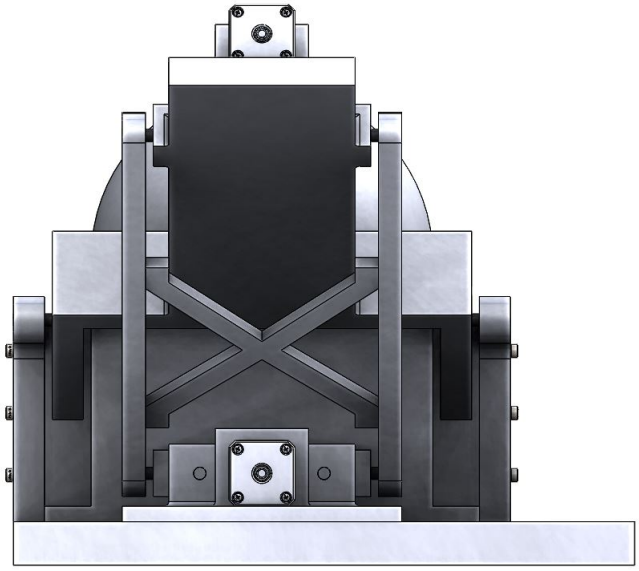

Figure 5.13: Back view of the system, where the cross-linkage is visible.

5.6. Required torque calculations

There are three different motions for which a stepper motor will be needed: the stepper motor to move the camera, the stepper motor to tilt the mechanism, and the stepper motor to rotate the object. The object that will be rotated will have a small mass, and most stepper motors will have sufficient torque to rotate the object. The required torque will therefore not be calculated. The torque needed to move the camera and tilt the mechanism will be calculated to select the right stepper motors for the system.

The equation to calculate the required torque with a leadscrew mechanism is shown in Equation 5.19 [27].

$$T = \frac{F \cdot d_m}{2} \cdot \left(\frac{l + \pi \cdot \mu \cdot d_m}{\pi \cdot d_m - \mu \cdot l} \right) \tag{5.19}$$

In Equation 5.19, F is the load in Newton, d_m is the mean diameter of the leadscrew in meters, μ is the coefficient of friction between the leadscrew and the leadscrew nut, and is dimensionless, and l is the lead which is in meters. This equation does not take the friction from the guiding axes into account. Therefore, a safety factor will be needed.

The approximate weight of the camera, lens, and mover is 0.25kg. With a friction coefficient μ of 0.2, a leadscrew with a diameter of 8mm and a lead of 2mm, the required calculated torque to move the camera is 0.003Nm. This is the required torque without taking into account the friction of the guiding axes.

The approximate weight of the tilt mechanism is 1.7kg. The required torque to tilt the mechanism will be calculated assuming that this load will completely support on the mover that tilts the mechanism. In reality, the load will be less because the tilt mechanism is also supported on the base. Therefore, the torque that will be calculated will be higher than needed. When calculating with a weight of 1.7kg, the required torque is 0.020Nm. This is the torque required to move a load of 1.7kg with a leadscrew without taking into account the friction of the guiding axes and ball bearings at the joints. However, in reality, a smaller load will be moved, so a safety factor is already included in this calculated torque.

Available NEMA17 Stepper motors typically can provide 0.5Nm torque when operating in full-stepping mode and cost around €14. This means that by using these stepper motors, a factor 25 higher torque

is available than needed in full-stepping mode. The same NEMA17 stepper motor will be used for all three motions because stepper motors with less torque are not much cheaper.

5.7. Stepper motor calculations and considerations

After choosing the stepper motor, the theoretical maximum speed can be calculated. The specifications of the chosen NEMA17 stepper motor are the following:

- **Maximum current per phase:** 1.8A.
- **Inductance:** 3.2 mH.
- **Steps per revolution:** 200.

The maximum speed of a stepper motor is limited by the time it takes for the coil to energize to its maximum holding current and then de-energize as polarity flips. The current that passes through the coil is proportional to the time the voltage has been applied and is inversely proportional to the inductance. This is expressed in Equation 5.20, where I is the current, V is the applied voltage, T is the number of seconds for a single step, and L is the inductance [8].

$$I = \frac{V \cdot T}{L} \tag{5.20}$$

Rewriting Equation 5.20 results in:

$$T = \frac{I \cdot L}{V} \tag{5.21}$$

For the stepper motor to make one step, the current must go from the maximum current I and back to 0. Therefore, I = 2 $\cdot I_{max}$. Filling this in Equation 5.21 results in:

$$T = \frac{2 \cdot I_{max} \cdot L}{V} \tag{5.22}$$

To compute the revolutions per minute (RPM), T, which is seconds per step, is divided by the steps per revolution. This will result in the number of revolutions per second. Multiplying this by 60 gives the RPM. A theoretical maximum RPM of 313 is calculated when the stepper motor is operated at full-stepping mode by filling in the corresponding values. This theoretical maximum speed will be reached if the stepper motor still provides enough torque at that speed.

However, the stepper motor can also be operated in micro-stepping mode instead of full-stepping mode. Micro-stepping provides several advantages such as reduced mechanical noise, gentler actuation mechanically, and reduces resonances problems. By micro-stepping, the torque of the stepper motor will be reduced significantly. At, for example, quarter stepping, the remaining torque is only 38.27%. The disadvantage of micro-stepping is that the maximum achievable RPM is less than when full-stepping. More steps per revolution need to be done, and less torque is available. Therefore, if the stepper motor is sufficiently mechanically damped by the way it is connected to the mechanism and no resonance effects are observed, full-stepping is desired to achieve higher RPM.

5.8. Stress analysis

Stress analysis was done on the critical components where the highest reaction forces are expected to ensure that the stress does not exceed the yield stress and cause permanent deformations. The critical components that were analyzed on the stresses that they are subjected to are the bottom mover and the connecting links. The bottom mover makes the mechanism tilt when the leadscrew is actuated. The upper part of the tilt mechanism supports on the bottom mover and the connecting links, apart from supporting on the connection with the base. Again, the assumption is made that the whole weight of the upper part of the tilt mechanism is supported on these components. If the stresses that are computed with that assumption are below the yield stress, then the real situation will also have stresses below the yield stress. However, 3D parts can be 3D-printed with different settings. The 3D-printed parts will not be printed solid. The 3D-print settings influence the material behaviour, and therefore the COMSOL calculations will not be completely accurate because the 3D-print settings are not considered. In Figure 5.14 the COMSOL simulations are shown where the stresses are computed. The maximum stresses computed by COMSOL are 0.07 MPa and 0.08 MPa for the bottom mover and the connecting link, respectively. The yield stress of PLA is 27 MPa, which means that the stresses are definitely not too high in the 3D-printed parts [1].

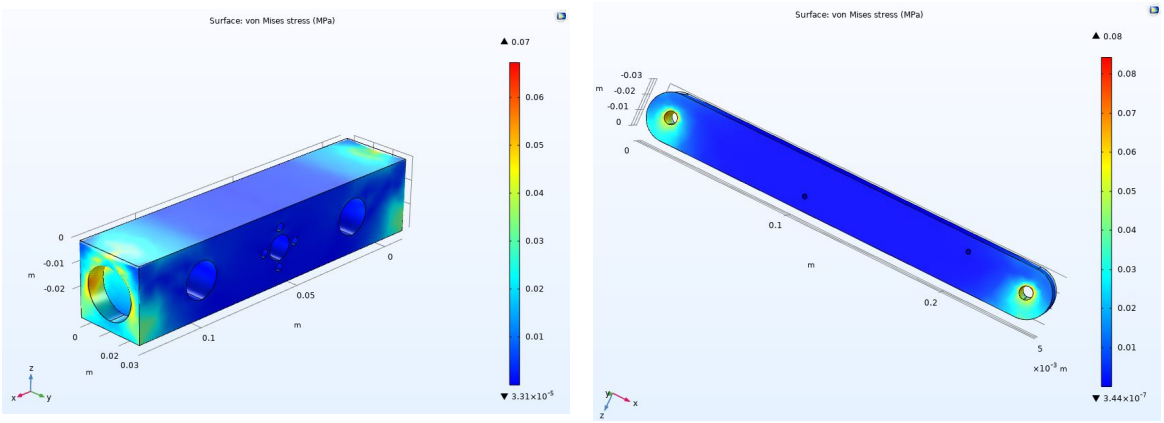

(a) (b)

Figure 5.14: Stresses computed with COMSOL for the critical components of the system. **(a)** Stresses in the bottom mover. **(b)** Stresses in the connecting link.

5.9. Stability considerations

The designed system is difficult to analyze analytically or to create a model to predict the level of stability that it will have. It is complex because the design has many components that are difficult to model, such as 3D-printed parts and connection elements with unknown behavior. Therefore, the design is difficult to model to predict stability. A model that predicts the stability of this system would be useful to improve the stability of the system further. However, creating such a model will be complex and time-consuming. The approach to design a stable system was by using engineering principles, such as creating a stiff design and implementing mechanical damping to reduce vibrations. This pragmatic approach is more time-efficient than creating a model. A prototype of this designed system will be made and evaluated.

5.10. Cost overview

In Table 5.1, a cost overview for the prototype is shown. The total cost is €486. Compared to the high-end solutions, which costs several thousands of euros, this is a cost-effective design.

Component	**Quantity**	**Total Cost** [€]
Raspberry Pi HQ Camera	1	42
Raspberry Pi 4B Microcontroller	1	60
Raspberry Pi 16mm Lens	1	50
Lens 3mm focal length 37mm OD	1	6
3D-Printed parts	1	65
Leadscrew TR8x2 30 cm	2	19
Leadscrew nut TR8x2	2	12
Flexible coupling 5mm-8mm	2	8
Steel axes	1	8
LM8UU linear ball bearing	6	7.50
Ball bearing 608ZZ	10	7.50
Glue	1	7
Stepper motor driver DRV8825	3	14
NEMA17 Stepper motor	3	42
Stepper motor cable	3	4
Jump wires and wire	1	5
LED strips 90 CRI, 4000K	1	9
Base plate	1	20
Power supplies	3	30
Fixing material (bolts, nuts, rings, inserts)	1	40
Other electronics	1	30
Total cost		486

Table 5.1: Total cost of the prototype of the designed system.

6

Prototype setup

In this chapter, the build prototype setup is shown and discussed. Firstly, the electronics involved, including the wiring diagram with the needed components and how the needed current is set for the stepper motors, are explained. Secondly, the assembly of the prototype will be demonstrated. Moreover, finally, the way the prototype setup was programmed with Python code to make photographs of the object from different angles will be discussed.

6.1. Electronics

In this subchapter, the active electronics in the prototype setup are discussed. First, the wiring diagram is shown with the needed components. Secondly, it is explained how the current is set for the stepper motors.

6.1.1. Wiring diagram

The following electrical components are needed to make the system function properly: a Raspberry Pi 4B microcontroller, a Raspberry Pi HQ camera, a breadboard, three DRV8825 stepper motor drivers, three 100 μF capacitance's, jump wires, copper wire, LED strips, and power supply's for the stepper motors, the Raspberry Pi 4B microcontroller, and the LED strips. In Figure 6.1, the wiring diagram is shown. The jump wires are connected to the Raspberry Pi 4B microcontroller to control the stepper motor drivers. The Raspberry Pi HQ camera is connected directly to the Raspberry Pi 4B microcontroller. The 100 μF capacitance's are needed to protect the driver from LC voltage spikes which can permanently damage the stepper motor drivers.

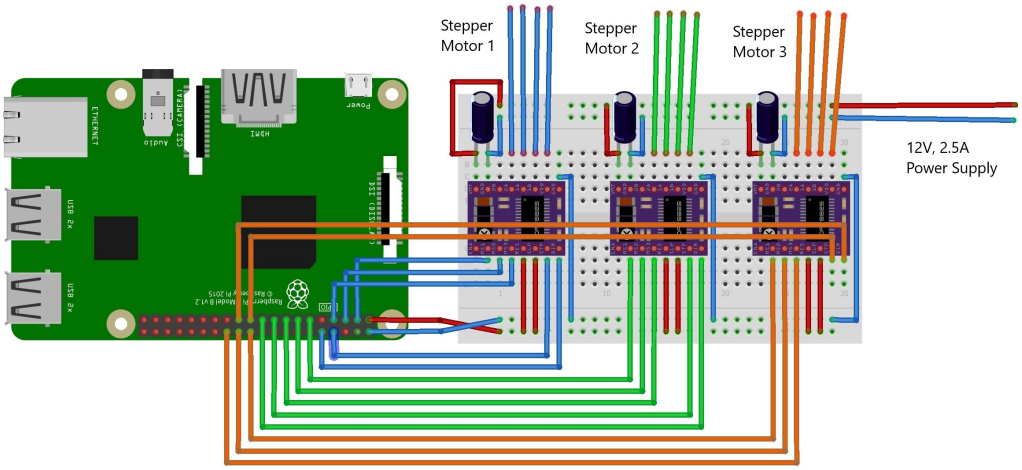

Figure 6.1: Wiring diagram of the prototype setup. On the left the Raspberry Pi microcontroller can be seen and on the right the stepper motor drivers.

6.1.2. Current supply stepper motors

Setting the current limit with the stepper motor driver is essential to make sure that it runs properly. By having an appropriate current limit, it is also ensured that the stepper motor or the stepper motor driver is not damaged by having a too high current [19]. Setting the current limit of the stepper motor driver is done by adjusting the on-board potentiometer. This can be done by using a multimeter to measure the voltage V_{REF} to set the current limit. Equation 6.1 shows the relation between the measured V_{REF} and the current limit. The maximum current per phase for the selected stepper motors is 1.8 A per phase. By using Equation 6.1, it can be determined that the maximum value for V_{REF} can be 0.9V. To not overheat the electronic components, the current limit will be set at 0.8V.

$$CurrentLimit = V_{REF} \cdot 2 \tag{6.1}$$

In Figure 6.2, it is shown how the current limit was set with the setup.

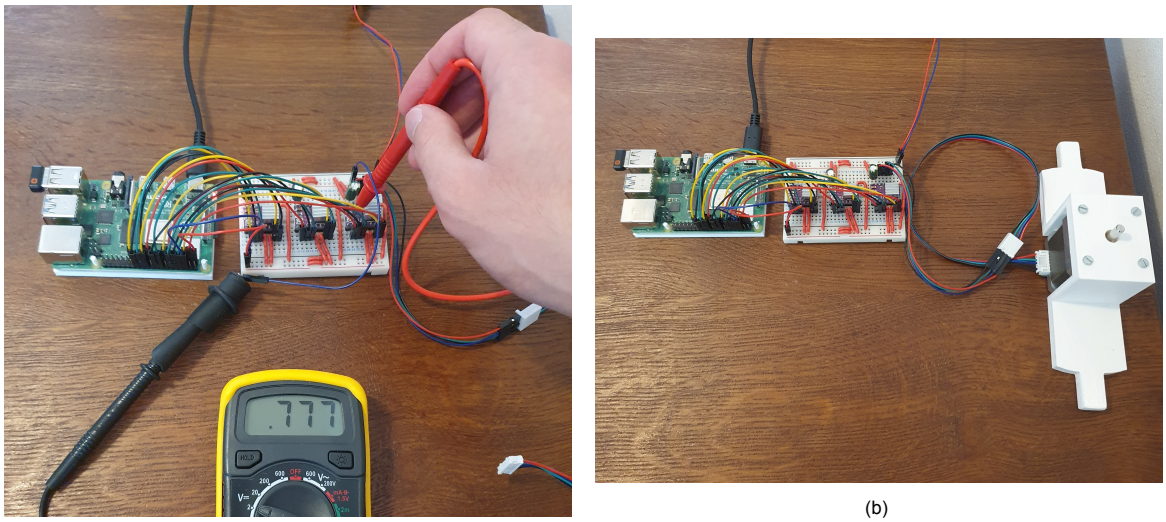

(a) (b)

Figure 6.2: This Figure shows how a multimeter was used to set the current limit for the stepper motor drivers. **(a)** Multimeter indicating approximately 0.8V via the potentiometer. **(b)** After setting the current limit, the stepper motor can be connected to the stepper motor driver.

6.2. Assembly

In this subchapter, the assembly of the prototype setup will be explained. The assembly steps are straightforward. In Figure 6.3, the individually assembled components of the system are shown, categorized by name. Most of the components were produced with a 3D printer. The following individual components are shown: the upper mover, the base with the bottom mover mounted, the connecting links, the light dome with the LED strips implemented, the turntable, and the connectors that are used to connect the upper mover to the base and to fix the light dome to the base.

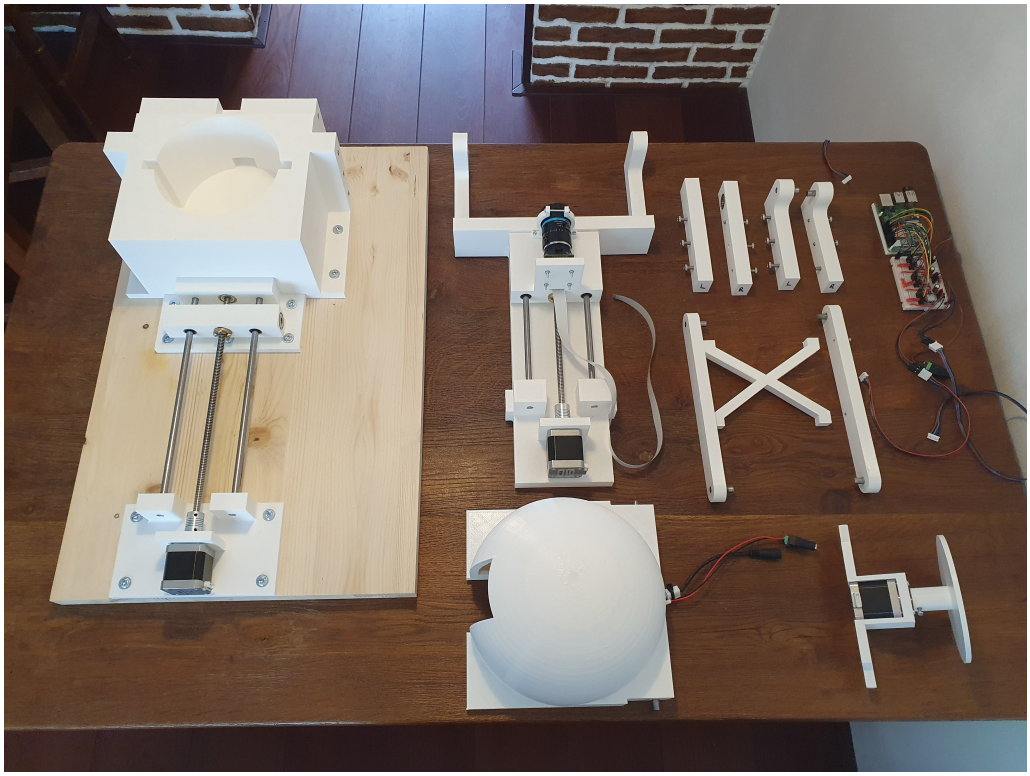

Figure 6.3: In this Figure, the individually assembled components of the system are shown that have been given a name to explain the assembly process.

The assembly steps are the following:

- Firstly, the upper mover is connected with the connectors to the base.
- Then, the upper mover is connected to the bottom mover with the connecting links.
- The connecting links are attached with bolts onto the cross-linkage to connect the upper mover and bottom mover.
- Afterward, the turntable is placed into the base.
- And finally, the light dome is fixed with the connectors to the base.

In Figure 6.4 and 6.5, the complete assembly of the prototype is shown.

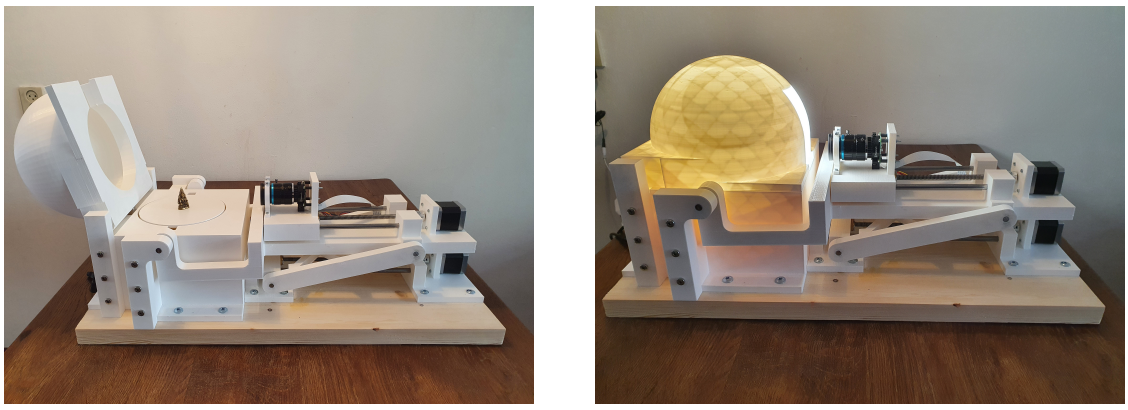

(a) (b)

Figure 6.4: This Figure shows the complete assembly of the prototype setup. **(a)** Prototype setup with the light dome up. **(b)** Prototype setup with the light dome down, ready to start to take photographs of an object.

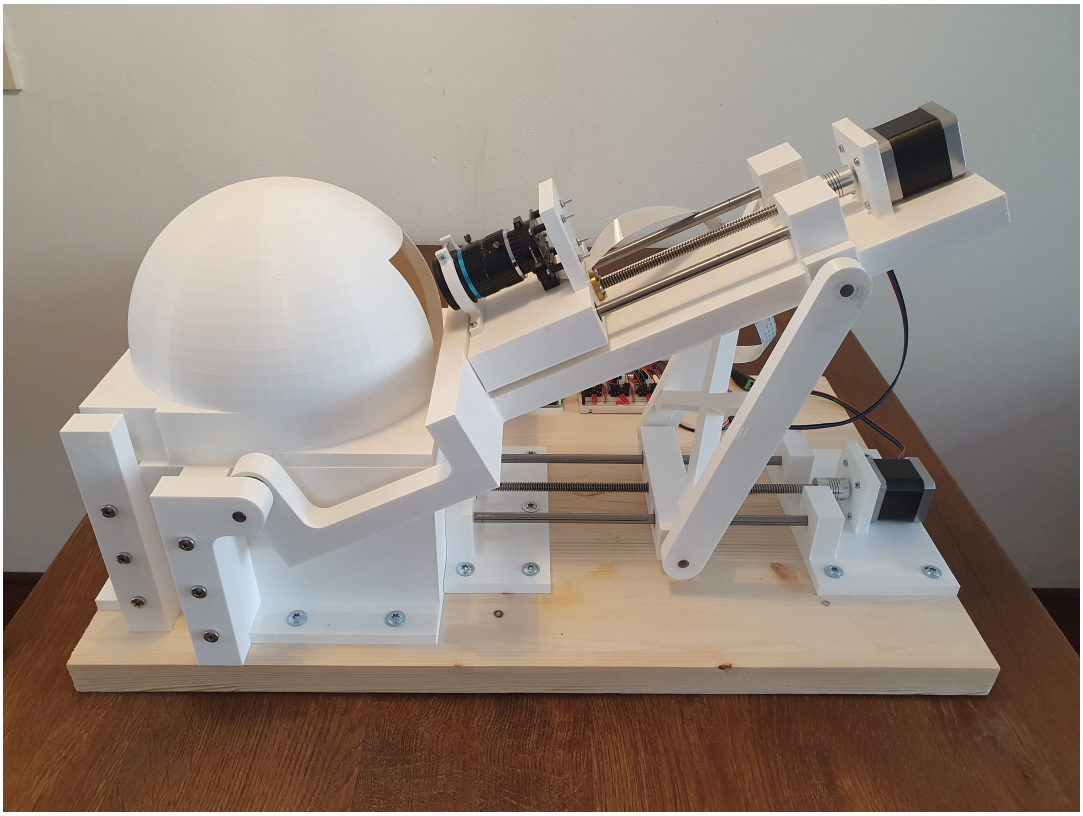

Figure 6.5: In this Figure, the complete assembly is shown in the tilted position.

6.3. Coding

A code in Python was written to make the prototype setup work and take photographs of the object. The code for the prototype works in the following way. Before starting to make photographs, it can be set how many tilt positions will be photographed and what the overlap percentage of the photographs will be. For each stack of photographs, a separate folder will be made where the photographs will be stored. The step size for focus stacking and the number of photographs per stack can be set manually. The Python code can be found in Appendix B.

7

Performance evaluation

In this chapter, the performance of the system is evaluated. Firstly, an overview of the involved variables that influence the system's performance is given and discussed. The considerations when configuring these variables, how the variables involved influence each other, and the resulting performance of the system are discussed. The performance evaluation approach is explained, and in the subsequent subchapters, different sub-systems, functions of the system, and resulting 3D-images are evaluated.

7.1. Overview of the variables involved

This subchapter will give an overview of the variables involved that influence the system's performance. It will be discussed how these variables affect each other and how they affect the system's final performance. The system's performance is defined by the quality of the created 3D-image and the time needed to acquire it. The variables involved can be categorized for the sub-systems that have been determined before in Chapter 4.6. In Figure 7.1, an overview of the different variables involved categorized per sub-system is given. The involved variables will be discussed per sub-system.

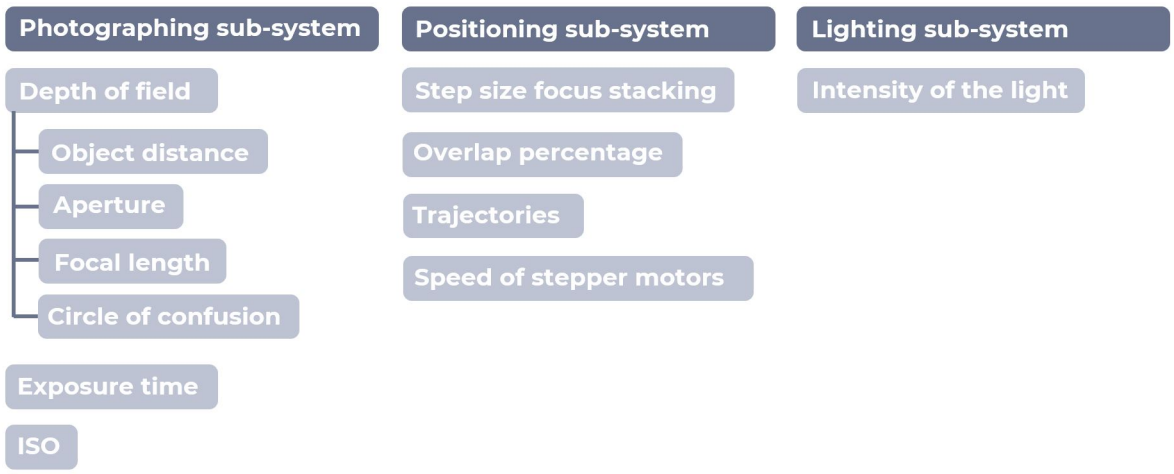

Figure 7.1: Overview of the variables involved that influence the system's performance categorized per sub-system.

Photographing sub-system:

The involved variables that affect the system's performance for the photographing sub-system are the following: the depth of field, the exposure time, and the ISO settings. The depth of field is dependent on the object distance, aperture, focal length, and the circle of confusion. Some of those variables on which the depth of field is dependent have been assigned a value in the process of designing the system. Those variables are the object distance, the focal length, and the circle of confusion. The only

real variable that is left to be configured is the aperture.

The aperture variable value influences the system's performance in the following way: the depth of field increases by having a small aperture. The depth of field increases because the rays converge better onto the image plane, causing fewer blur spots, illustrated in Figure 7.2. The downside of having a smaller aperture is that less light is let through onto the camera sensor, resulting in a darker photograph. By making the radius of the aperture two times smaller, the effective area of the aperture becomes four times smaller, resulting in four times less light. The exposure time or the ISO value has to be increased to increase the amount of light that is let through onto the sensor.

The exposure time is the amount of time the sensor is exposed to the light. The ISO value is the sensitivity of the camera sensor to light. By having a smaller aperture, resulting in a bigger depth of field, fewer photographs are needed to create a stack of photographs where all the object parts are in focus. This can potentially result in a faster system. If the exposure time was already short compared to the time needed to take a step to make the following photograph, then it can become a faster system by making the aperture smaller and increasing the exposure time. If the exposure time were long compared to the time needed to take a step to make the following photograph, then it would not result in a faster system by making the aperture smaller and increasing the exposure time. In that situation, instead of increasing the exposure time, if the ISO value is increased, it would result in a faster system. If the exposure time had to be increased after making the radius of the aperture two times smaller, the exposure time would have to be multiplied by four to get the same light. This would result in a slower system if the exposure time were long before making the aperture smaller. Therefore, the ISO value should be increased instead of the exposure time to create a faster system. The disadvantage of increasing the ISO is that it causes noise on the made photograph, resulting in a lower quality photograph. Also, the aperture should not be too small. A smaller aperture will increase the depth of field, but a too-small aperture could soften the overall sharpness of the photograph due to diffraction.

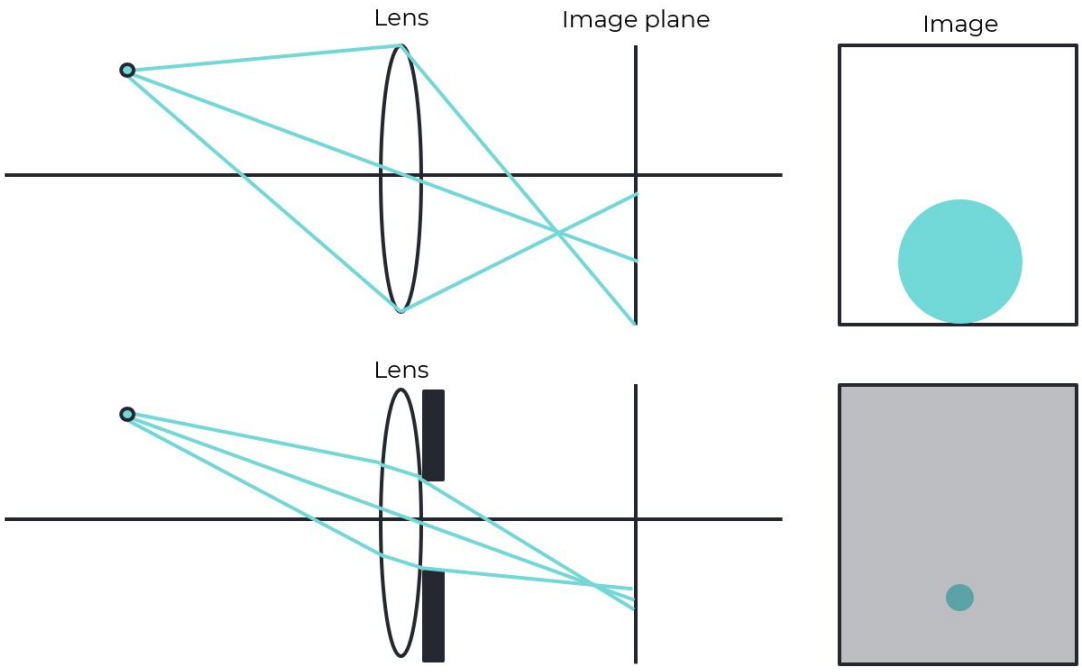

Figure 7.2: A simplified illustration to show the relationship between the aperture and depth of field. By using a small aperture, the light rays get bent narrower, resulting in a smaller bundle of light rays on the image plane that can fall within the circle of confusion and reducing blur. The downside is that the image will be less illuminated without increasing the exposure time or ISO value.

Positioning sub-system:

The involved variables that affect the system's performance for the positioning sub-system are the following: the step size used for focus stacking, the overlap percentage between photographs, the trajectories used to take photographs, and the speed of the stepper motors. The step size used for focus stacking is determined by the depth of field. The step size should be equal to the depth of field, or smaller than the depth of field, to ensure that all the object's parts are photographed in focus in the individual photographs. This is depicted in Figure 7.3.

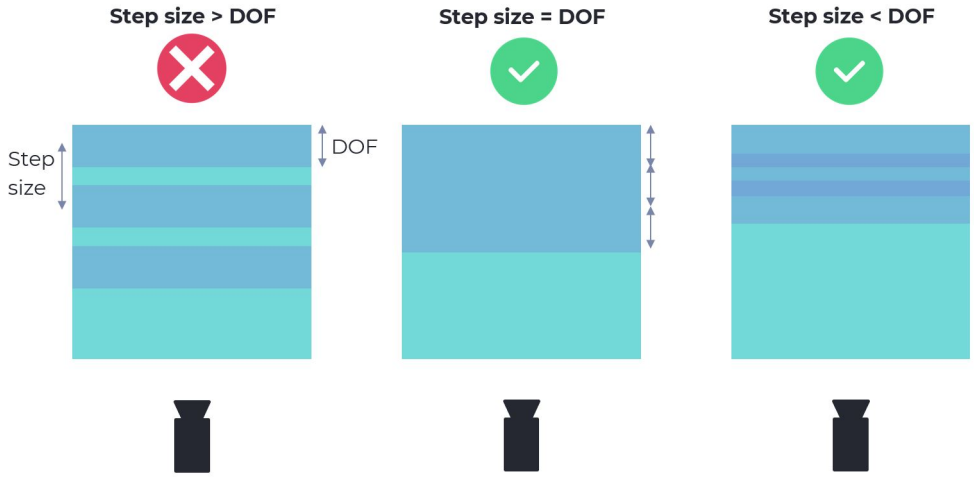

Figure 7.3: Step size for focus stacking consideration. The step size should be equal or smaller than the depth of field at the furthest point of focus to capture the object completely in focus.

The overlap percentage between photographs is another important variable that can be configured considering the positioning sub-system. A higher overlap percentage will make it easier for the photogrammetry software to identify identical feature points to create a 3D-image and will result in a higher quality 3D-image. A high overlap percentage means more photographs will be made of the object, resulting in a longer time needed to acquire the photographs of the object. Equation 7.1 is used to calculate overlap percentage. In Figure 7.4 an illustration is shown on how the overlap percentage is calculated.

$$OP = \frac{180 \circ - \alpha}{180 \circ} \tag{7.1}$$

Here α is the rotational step size in degrees that corresponds to a certain overlap percentage OP.

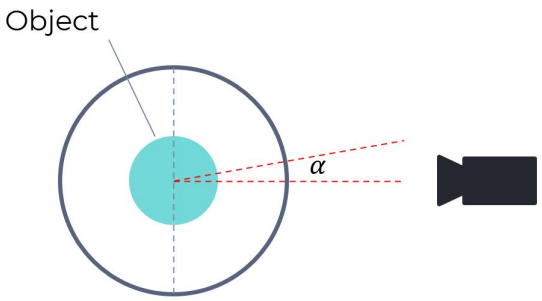

Figure 7.4: In this Figure, a top view of the object and turntable illustrates how the overlap percentage is calculated. The overlap percentage is calculated by subtracting the angle α, which is the rotational step size of the 180 °visible of the object before moving to the next position and dividing it by 180 °.

One more variable involved in the positioning sub-system is the number of trajectories to take photographs of the object which is related to the overlap percentage. By following more trajectories to take photographs of the object, more angles of the object will be photographed, and more photographs will be taken in general. By doing so, a higher quality 3D-image can be created with the photogrammetry software for the same reason as mentioned before.

With the trajectories variable, there also has to be made the decision of whether the camera is tilted first for each angle of the object or if the object is first rotated and photographed and then tilted. To have a faster system, it is better to rotate the object at each tilt angle of the camera. This is because the stabilization time when tilting the mechanism is higher than when moving the camera at a fixed tilt angle. This is because the amount of mass moved when the mechanism is being tilted is much higher than when the camera is moved at a fixed tilt angle. This results in a bigger moment of inertia and larger reaction forces in the mechanism, resulting in bigger vibrations and a longer stabilization time when the mechanism is being tilted than when the camera is being moved, which has a lower mass.

The last variable for the positioning system that has to be discussed is the speed of the stepper motors. The highest possible speed while maintaining stability is desired. The maximum speed of the stepper motors is determined by the applied voltage, if micro-stepping or full-stepping is applied, and the torque of the stepper motor.

Lighting sub-system:

For the lighting sub-system, there is only one variable that can be configured: the intensity of the light. High intensity of the light is desired to illuminate the object well. Because the designed system has a diffused lighting setup, high intensity of the light will not cause strong shadows and strong reflections. High light intensity is also desired because it can reduce the exposure time. That is because more light is projected onto the camera sensor. High light intensity makes it possible to keep a low ISO and use a smaller aperture to increase the depth-of-field.

7.2. Performance evaluation approach

The performance evaluation approach will be in the following way. Firstly, separate sub-systems and functions of the system will be evaluated. These include the guiding mechanism, focus stacking, and stepper motor settings. Finally, two 3D-images will be created of the same object. One 3D-image with ”minimal” settings, where a 3D-image will be created as fast as possible that will create a minimal result. And one 3D-image with the ”best” possible settings, where more time will be needed to acquire the photographs and to create the 3D-image with the photogrammetry software. With the best possible settings is not meant optimal settings, but settings that will guarantee a good result for the created 3D-image. By creating those two 3D-images mentioned, the extremes are shown, which can be achieved with this system. Further optimization can be done to find an optimal 3D-image between the minimal quality 3D-image and best quality 3D-image regarding the quality of the 3D-image and the time needed to acquire it.

7.3. Guiding mechanism

The guiding mechanism has been tested. The guiding mechanism is driven by applying torque with the stepper motor. The guiding mechanism is used to move the camera and tilt the mechanism. The guiding mechanism works well for the camera's movement and for the movement of the tilting mechanism. However, the mechanism sometimes jams and makes a loud mechanical noise. This is because the flexible coupling is too flexible, causing the leadscrew axis to move around its axis and move somewhat outward. This outward movement of the leadscrew axis causes grinding between the leadscrew, the leadscrew nut, and the flexible coupling. As a result, it makes a loud mechanical noise, and the mechanism jams sometimes. This problem can be solved by applying another support point near the end of the stepper motor with another ball bearing. By doing so, the outward movement is constrained, and the mechanism can work smoothly. In Figure 7.5, the problem with the guiding mechanism is depicted.

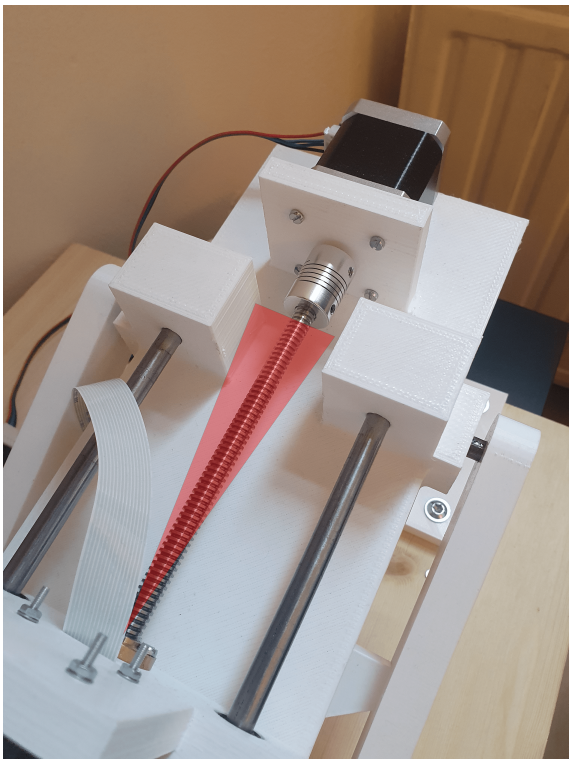

Figure 7.5: This Figure illustrates the problem with the guiding mechanism. The red area is the exaggeratedly drawn workspace to indicate how the leadscrew axis moves sometimes and causes mechanical noise, and causes the mechanism to jam.

7.4. Focus stacking

In this subchapter, the quality of the made photographs will be discussed together with the quality of the focus stacked image. Two different focus stacking methods will be used and compared, namely the weighted-average method and the Laplacian pyramid method that has been discussed in Chapter 2.

In Figure 7.6, the photograph with the furthest point of the object in focus is shown. The object is approximately 4cm long and 2cm wide. The camera is then moved, and multiple photographs are taken where different parts of the object are in focus. These photographs are stacked together to create a high-resolution image of the object. The photographs were made with the largest aperture that the lens has available.

Figure 7.6: Photograph of the object with the furthest point in focus. This object has a length of 4 cm and width of 2 cm.

Figure 7.7: Focus stacked image of the object with the Laplacian pyramid method.

In Figure 7.7, the result of focus stacking the made photographs of the object is shown. This result was achieved with the Laplacian pyramid method to focus stack the photographs, which ultimately gave the best result. In Figure 7.8, the results of the focus stacked image for the weighted-average method and the Laplacian pyramid method are shown. From subjective visual evaluation, it can be seen that the weighted-average method results in blurry lines and a weird glow around the object. The Laplacian method does not have this issue and creates a higher quality focus stacked image.

(a) (b)

Figure 7.8: The result of focus stacking the photographs of the object with two different methods. **(a)** The weighted-average method. **(b)** The Laplacian pyramid method.

It can also be observed that the field of view of the camera corresponds to the calculated field of view in Chapter 5.2. From the made photographs and created focus stacked images, it can be seen that photographs have good lighting where no strong shadows, glares, and reflections are visible. From this, it can be concluded that the light dome setup that creates diffused light to illuminate objects is a robust lighting method.

7.5. Stepper motor settings

The stepper motor settings can be configured in the following way. The stepper motor can be set to full-stepping mode or micro-stepping mode. The advantages of using micro-stepping mode are better resolution, smoother motion, and reduced resonance. The disadvantage of using micro-stepping mode is that the torque of the stepper motor reduces significantly, and therefore the speed that the motor can reach is also reduced.

For the movement of the camera and the tilt mechanism, full-stepping mode is set. This is because when experimenting with full-stepping mode, smooth motion was observed. No resonance effects were observed when operating at full-stepping mode, this is probably because the stepper motors are loaded and connected with the mechanism. This ensures mechanical damping and reduced resonance effects.

For the rotation of the turntable, the stepper motor is set to micro-stepping mode. This is done to reduce the torque to ensure that the torque does not become so high that it can displace the object on the turntable.

7.6. 3D-Images

In this subchapter, two created 3D-images are shown. One 3D-image with ”minimal” settings, where a 3D-image will be created quickly that will create a minimal result. And one 3D-image with the ”best” possible settings, where more time will be needed to acquire the photographs and to create the 3D-image with the photogrammetry software. For the 3D-image with the minimal settings, low overlap percentage, and less trajectories will be used. For the 3D-image with the best settings, high overlap percentage, and more trajectories will be used. Due to camera issues with the Raspberry Pi 4B microcontroller, the exposure time and ISO could not be configured to experiment with. The camera was, therefore, only able to operate on automatic settings. Otherwise, for the minimal settings, there could be experimented with the aperture and ISO, to acquire the photographs even faster. This would come at the cost of a lower quality photograph with noise, but it would suit the 3D-image with ”minimal” settings.

The acquisition of the photographs for the 3D-image with the ”best” settings took 60 minutes. 1200 Photographs were made, 10 photographs were made for each position, which resulted in 120 stacked images. An overlap percentage of 95% and 2 tilted position were used. The acquisition of the photographs for the 3D-image with the ”minimal” settings took 10 minutes. 200 photographs were made, 10 photographs for each position, which resulted in 20 stacked images. An overlap percentage of 80% was used and 1 tilted position was used. The post-processing time required to create the 3D-image with the ”minimal” settings was 20 minutes and to create the 3D-image with the ”best settings was 180 minutes. The speed of the photographs acquisition was not limited by the stabilization time of the camera but by the time needed to make and save the photograph. The system stabilized faster than the exposure time, because no visible motion blur was observed when photographing with the Raspberry Pi HQ camera with automatic settings. The total time needed to create the 3D-image with the ”best” settings was 240 minutes, or 4 hours. And the total time needed to create the 3D-image with the ”minimal” settings was 30 minutes, or half an hour. In Figure 7.9, the result of the created 3D-image with the ”best” settings can be seen and in Figure 7.10 the result of the created 3D-image with the ”minimal” settings.

By subjective visual evaluation of the two created 3D-images, intuitively it can be seen that the 3D-image created with the ”best” settings provides a much higher quality. The 3D-image of the object is complete with high-quality texture and color information. In the 3D-image with ”minimal” settings, holes in the object can be seen and is incomplete. The 3D-image of the object looks distorted. The 3D-image also contains unwanted elements that do not belong to the object.

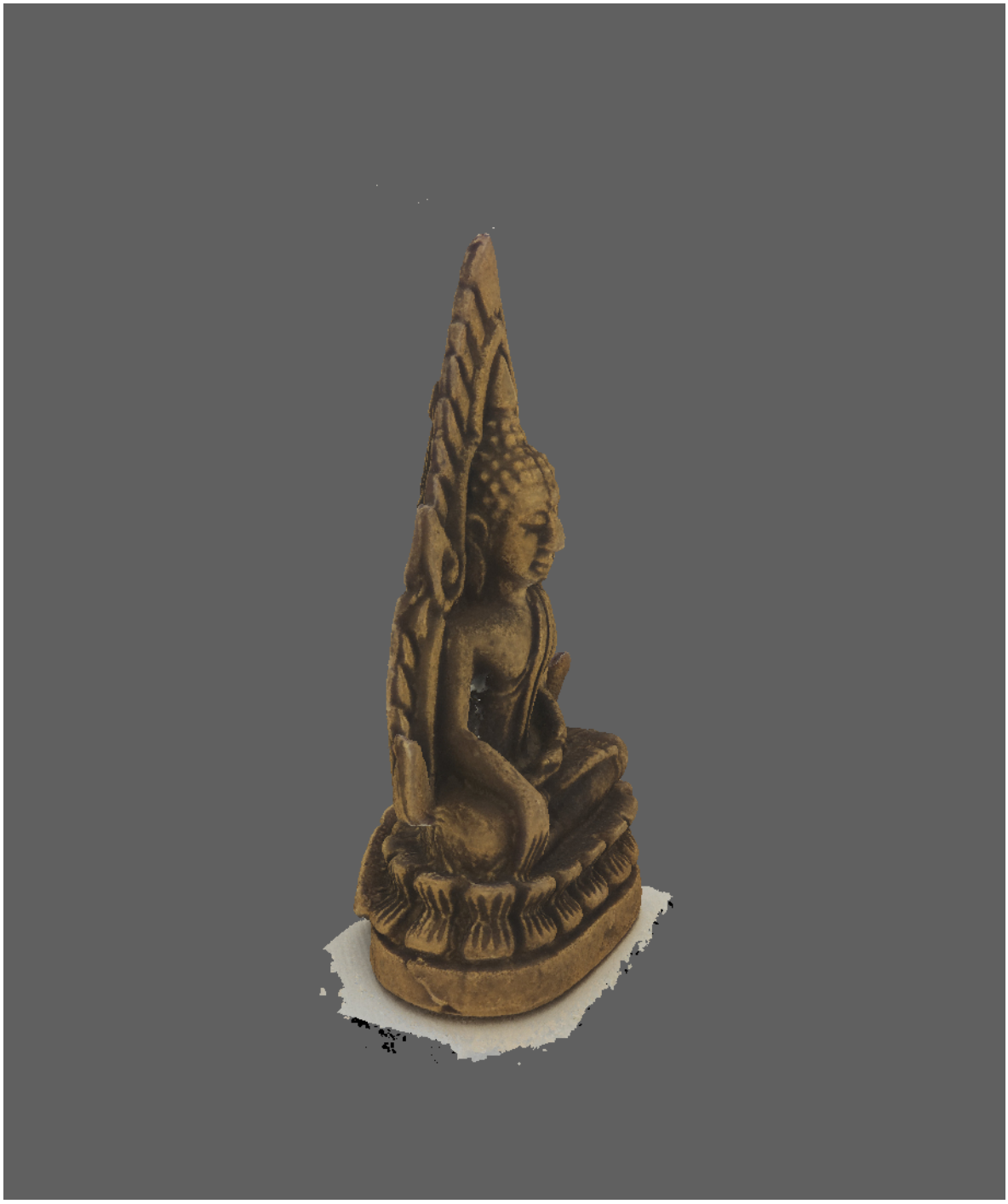

Figure 7.9: 3D-image created with the ”best” settings. 60 Minutes were needed to acquire the photographs, and 180 minutes were needed to post-process the photographs to create the 3D-image. Click the figure to be able to move the 3D-image.

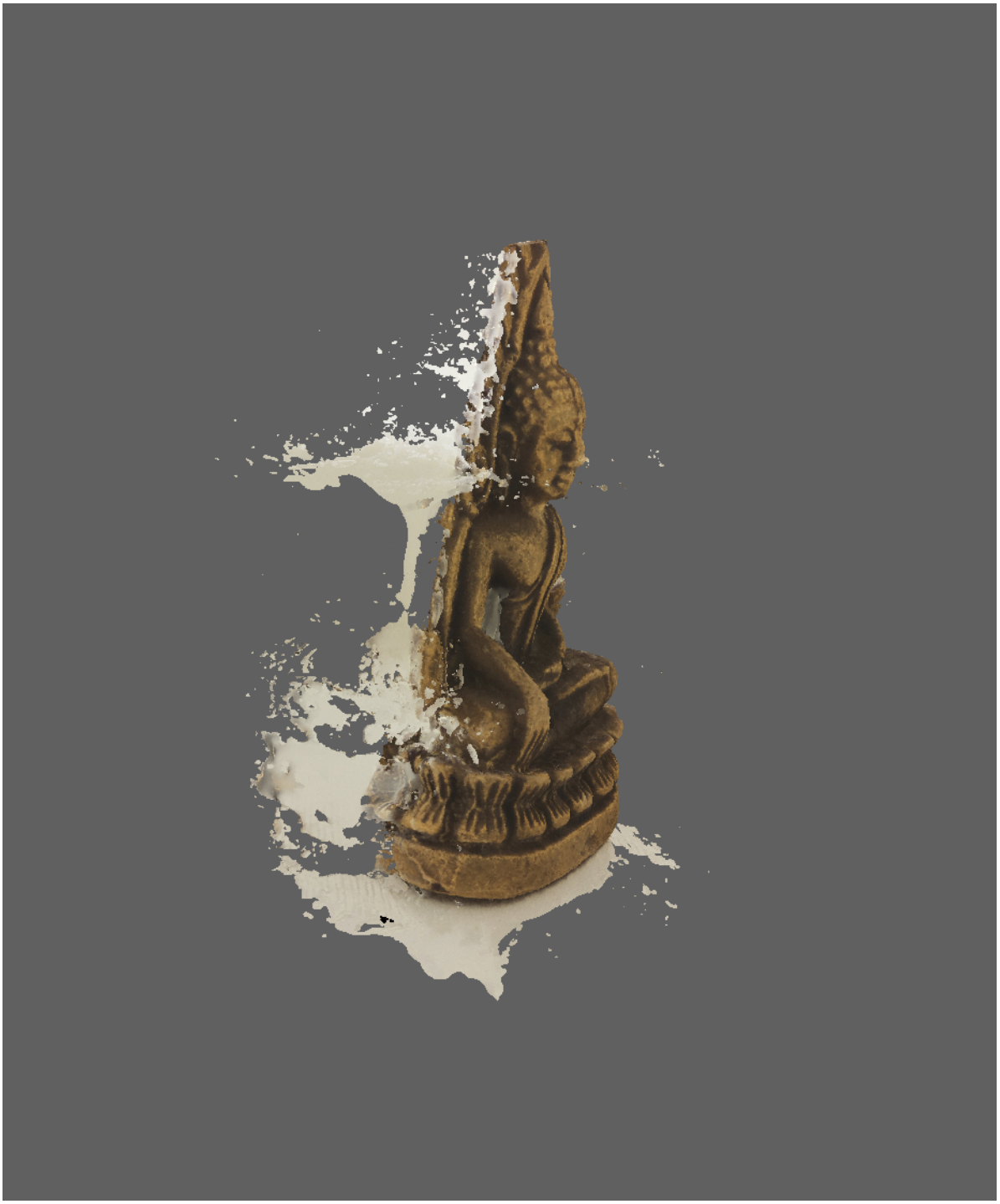

Figure 7.10: 3D-image created with the ”minimal” settings. 10 Minutes were needed to acquire the photographs, and 20 minutes were needed to post-process the photographs to create the 3D-image. Click the figure to be able to move the 3D-image.

8

Conclusion and future work

This project can be concluded in the following manner. In this project, 3D-imaging technologies have been studied to choose the most suitable 3D-imaging technology for small archaeological artifacts to create a cost-effective 3D-imaging system that heritage institutions can use. Photogrammetry has been found to be the most suitable 3D-imaging technology, mainly because of its ability to create detailed textures and color information of the object. Photogrammetric 3D-imaging systems have been studied on their ability to automatically create high-quality 3D-images. Literature states that the quality of the 3D-images created with photogrammetric 3D-imaging systems suffers from a small depth of field. By the nature of optics, this small depth of field occurs when photographing an object from a close distance.

The main conclusions of this project are the following. A cost-effective photogrammetric 3D-imaging system for small archaeological artifacts was successfully designed and validated. This system is optimized for the depth of field and is able to successfully create high-quality 3D-images with highly detailed textures and color information, which serves several important purposes. This design overcomes the small depth of field limitations by implementing focus stacking. The system's most intensive task, the acquisition of photographs, has been automated, and a working compact system has been created. The system, as it is, is ready to be used by others. The designed system creates higher-quality 3D-images compared to other cost-effective solutions. Compared to expensive systems, the designed system creates 3D-images of comparable quality. However, the time to acquire the 3D-image with the designed system is significantly longer compared to expensive systems, approximately 5 times longer. The final cost of the designed system is below €500. Compared to other high-end solutions, which can be in the range of several thousands of euros, the designed system is much cheaper.

The designed system was achieved in the following way. For the design of the system, the necessary conceptual design was done. A flowchart was made that demonstrates how the system is intended to be used. The system's requirements have been set, and the challenges involved with designing such a system have been addressed. A concept was generated, and a detailed system was designed afterward. A prototype of the design was successfully built, and results were obtained. A 3D-image with the ”best” settings and a 3D-image with the ”minimal” settings were created. The 3D-image with the ”best” settings is high-quality, where the object's texture is highly detailed, and color information is preserved. The 3D-image with the ”minimal” settings showed a distorted 3D-image of the object. The quality of the texture was good, but not enough identical feature points were found by the photogrammetry software, resulting in a distorted 3D-image with holes. The total time needed to create the 3D-image with the ”best” settings was 240 minutes or 4 hours. Furthermore, the total time needed to create the 3D-image with the ”minimal” settings was 30 minutes or half an hour.

The designed system creates high-quality 3D-images and can be used as it is. However, the designed system can be improved in the following way. The recommendations for future work are categorized for the automation, the mechanism design, and the optimization of the system.

Recommendation considering the automation:

- **Automation of post-processing:** For the system to be used by heritage institutions, the system should be as automated as possible. The automation level of the system is indicated in Chapter 4. To achieve this, the post-processing part of the workflow should be automated. This includes automating focus stacking, implementing the stacked images in the photogrammetry software, and creating the 3D-image with the photogrammetry software.

Recommendations considering the mechanism design:

- **Material use:** The designed system is mostly 3D-printed. The time to 3D-print the parts is around 150 hours. To reduce the production time of the system, several large 3D-printed parts could be redesigned with of the shelf parts, like aluminium profiles. Only complex parts like the light dome should then be 3D-printed. Aluminium has a higher density than PLA, so it must be carefully considered when redesigning the parts. It must considered to make sure that the motors are able to provide the needed torque, or more powerful motors should be considered, which would make the system more expensive.
- **Calibration:** To calibrate the system and make up for step losses if they occur with the stepper motors, micro-switches could be used to calibrate the system.
- **Actuator choice:** Consider using a servo to move the camera. By doing so, a higher speed can be achieved since servos can operate at higher RPM and still provide enough torque. Since the torque required to move the camera is low, perhaps a cost-effective servo can be integrated into the system.
- **Multiple lens configuration:** With the current design, an object with a length and width of 2cm will still not utilize the camera sensor completely. A multiple lens configuration can be considered, where objects with a length and width of 2cm are photographed with another lens to zoom in on the object completely.

Recommendations considering the optimization:

- **Focus stacking:** With the built prototype, the same amount of photographs are taken at each position. To create a faster system, focus stacking should be optimized. This should be done so that only the necessary amount of photographs are taken per position. To do this, the geometry of the object should be known at the beginning. This could be achieved by adding a cost-effective laser triangulation scanner that calculates the geometry of the object.
- **Optimal 3D-image:** In the performance evaluation two 3D-images were shown, one with the ”best” settings and one with the ”minimal” settings. The time difference in creating these 3D-images is 3 hours. To further optimize the 3D-imaging process, an optimum regarding quality of the 3D-image and needed time to acquire it could potentially be found. This can be done by experimenting with different overlap percentages, amount of trajectories, and use of marker patterns. By creating 3D-images with different settings and evaluating them subjectively and objectively with quantitative analysis, an optimum could be found.
- **Camera programming:** The camera should be programmed better, to experiment with different apertures, exposure times, and ISO settings to further optimize the system. Also, the camera should be programmed to save photographs quicker to speed up the system.
- **Flash light concept:** Explore the possibilities to create an even faster system by using flash light with the diffused lighting setup. By using light with high intensity for a short amount of time, short exposure times can be achieved and potentially create a faster system.
- **Custom PCB:** Discover the possibilities to design a cost-effective custom PCB. By doing so, higher voltages can be used to operate the system at higher speeds, resulting in a faster system.

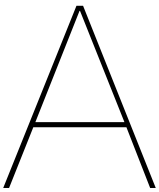

Literature study

Delft University of Technology

ME-HTE Literature Survey

ME56010

Research into the state-of-the-art 3D-imaging to create 3D-images of small archaeological artefacts

Author:

Marcos Alvarez (4377923)

January 4, 2021

MSc program Mechanical Engineering - Track in High-Tech Engineering

Contents

1 Introduction

The 3D-digitisation of precious cultural heritage artefacts is highly important for historical preservation purposes. By doing so, it can help mitigate against events such as tourism damage, natural disasters, and war. It also enables access to three-dimensional data for researchers all around the globe. This boosts historical research, researchers of all disciplines can work on the same object at the same time. Digital 3D-models of these artefacts enable us to study them without subjecting the fragile originals to danger. It is desired to capture these small archaeological artefacts as accurately as possible. Future generations would benefit from such an online database of 3D-models of small archaeological artefacts to study the history and understand it.

Currently, several high-end solutions are available to digitize the archaeological artefacts. One of them is the conveyor system by CultLab3D [1]. It utilizes different 3D-imaging technologies and can create a high-quality 3D-model of archaeological artefacts in a fast way. Although this is a sophisticated solution, the cost to purchase or leasing can be too substantial for many heritage institutions that often run on small budgets [2]. Therefore, there is a need for cost-effective solutions to create 3D-models of small archaeological artefacts.

The scope of this literature survey is to identify the existing 3D-imaging technologies and choose the most suitable technology to create high-quality 3D-models of small archaeological artefacts. With high-quality 3D-models are meant 3D-models where great attention has been paid to the development of a high-quality texture capable of keeping all the surface information. With these highly detailed textures with the color information of the object, a realistic impression can be generated of the object. The most suitable technology will then be further researched on the ability to create high-quality 3D-models of small archaeological artefacts in an optimized and cost-effective way. Existing systems and available knowledge will be researched to identify a knowledge gap and a possible improvement to existing systems. This report will be concluded with a proposal to improve an existing device to create 3D-models cost-effectively and optimally.

2 Background of 3D-imaging

3D-imaging is the technology of capturing the shape of an object to construct a 3D-model. It is the process of analyzing an object from the real world, to collect all the three-dimensional data in order to recreate its shape and appearance digitally [3]. There exist different 3D-imaging technologies that achieve the construction of a digital 3D-model. Each of these technologies has its advantages and limitations.

In the following section, these 3D-imaging technologies will be discussed and compared. Also, existing devices that make use of the 3D-imaging technologies will be discussed and compared. The goal of this chapter is to identify the existing 3D-imaging technologies and choose the most promising technology to create 3D-models of small archeological artefacts. This chosen technology will then be further researched on the ability to create high-quality 3D-models of small archeological artefacts in an optimized and cost-effective way.

2.1 Existing 3D-imaging technologies

The existing 3D-imaging technologies can be divided into "contact type" and "non-contact type". Contact type 3D-imaging technologies touch the object to obtain data about the shape of the object to construct a 3D-model. Non-contact type 3D-imaging technologies obtain data about the shape of the object without touching the object [4]. These different types of 3D-imaging methods can be further categorized by different contact and non-contact type 3D-imaging technologies. The different non-contact technologies can be further classified as active and passive methods. These categories can be further broken down into spot, pattern, and image. They will be further discussed in separate sections. Figure 1 shows a schematic representation of the available technologies to construct a 3D model.

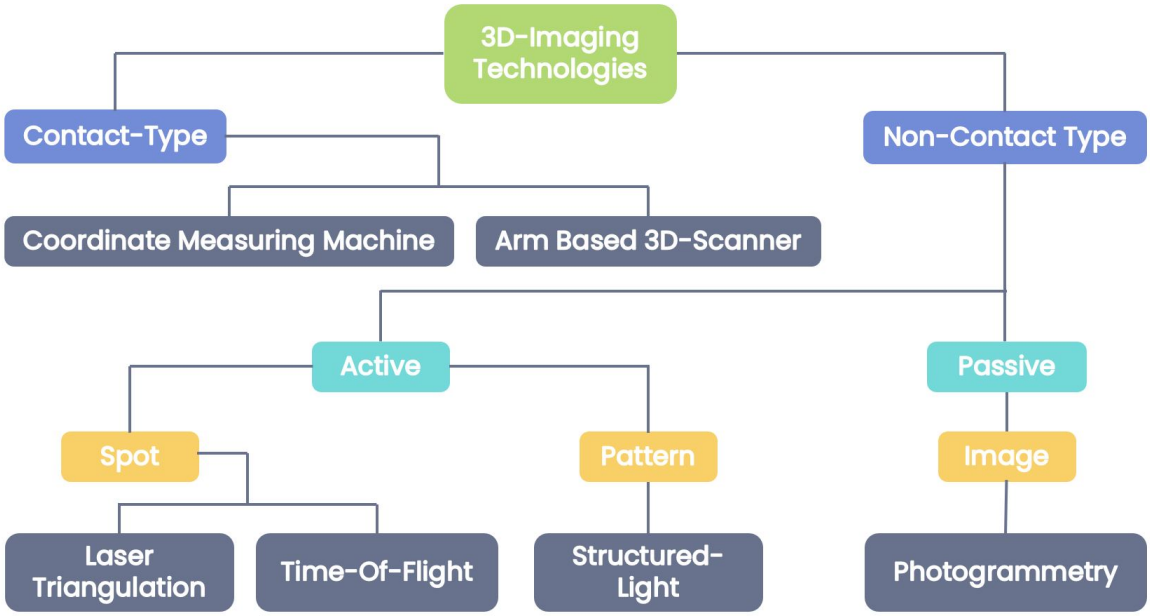

Figure 1: Overview of the different 3D-imaging technologies.

2.1.1 Contact type 3D-imaging

Contact type 3D-imaging technologies capture the shape of the object by touching it with a physical probe. With this method of 3D-imaging, the object that is scanned is either held stationary or moving, depending on the device [5]. The software that is used with this 3D-imaging technology keeps track of the movement of the device. It stores the three-dimensional data where the probe has touched the object to create a 3D-model [6].

This form of 3D-imaging has different advantages and disadvantages. One of the major advantages is that this 3D-imaging technology can scan reflective and transparent objects. Another advantage of this technology is that it is one of the most accurate technologies available, as it can perform 3D-imaging with an accuracy of a few microns. One more advantage is that small to large parts can be 3D-scanned with this technology.

The disadvantages of this technology are that it can be a time-consuming process and that the process is highly sensitive to movements and vibrations during the imaging [7] [8]. Another disadvantage of this 3D-imaging technology is that the object could potentially be deformed by the probe by touching it. This means that this technology cannot be used with objects that are easily deformed. One more disadvantage is that this 3D-imaging technology produces low-resolution data [9]. Contact 3D-scanners are primarily used in quality control [8]. There are two different ways contact type 3D-imaging technologies are applied, namely with a coordinate measuring machine (CMM) or an arm based 3D-scanner. They will be further discussed separately.

2.1.1.1 Coordinate measuring machine

One of the existing technologies that use contact type 3D-imaging is the coordinate measuring machine (CMM). The CMM has a physical probe that touches the stationary object to obtain three-dimensional data of the object. The CMM is primarily used to inspect parts and can be operated manually or it can be controlled through a computer. In the latter case, the CMM is programmed to touch the object. When the object is touched and sensed by the probe of the machine, a measurement value that is sampled in XYZ space is stored. To achieve an accuracy of a few microns, the CMM is operated in a very controlled inspection room [7]. The price of a CMM can range between $30K and $1M dollars, depending on the specifications [10]. In Figure 2a an example of a CMM is shown.

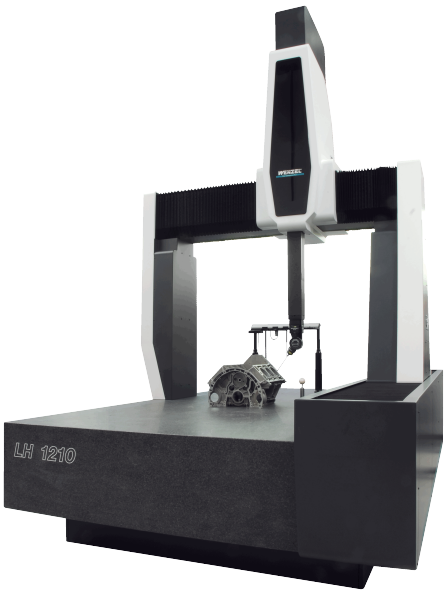

(a) Example of a CMM [11].

(b) Example of an arm based 3D-scanner [12]

Figure 2: An example shown of a contact type CMM and arm based 3D-scanner.

2.1.1.2 Arm based 3D-scanner

Another existing technology that uses contact type 3D-imaging is the arm based 3D-scanner. It works similar to the CMM mentioned earlier as it also uses a touch probe to measure the object. The arm based 3D-scanner works by attaching the arm to a table or a sturdy base. The arm is then manually controlled with a handgrip at the end of the arm. The software keeps track of the movement of the joint to create a 3D-model of the object. In Figure 2b an example of a contact type arm based 3D-scanner can be seen. The most important advantages and disadvantages of this technology were mostly already mentioned. Another main advantage of this technology specifically is that it is much more portable than the CMM, but in return, the accuracy of this technology is lower. The arm based 3D-scanner also does not need to be operated in a very controlled inspection room [7].

2.1.2 Non-contact type 3D-imaging

As mentioned before, the 3D-imaging technologies can be divided into contact type and non-contact type 3D-imaging. In general, the advantage of non-contact type 3D-imaging technologies is that they do not have to touch the object, thus preventing physical damage to the object. It is a less invasive way to make a digital 3D-model of an object. In this section, the available non-contact type 3D-imaging technologies will be discussed. They can be categorized by laser triangulation, structured light, time of flight, and photogrammetry.

2.1.2.1 Laser triangulation

Laser triangulation 3D-scanners use the trigonometric triangulation process to capture the 3D shape of an object as millions of points. They work by projecting multiple lines or a single laser line onto an object. The reflection of these laser lines can then be captured by a sensor or multiple sensors that are placed at a known distance from the laser source. By doing this, accurate measurement can be done by calculating the reflection angle of the laser light [7] [13].

The advantage of this 3D-imaging technology is that it can offer high resolution and accuracy, and it can perform a 3D-scan relatively fast in the order of tens of micrometers. Another advantage is that this process can be automated. A disadvantage of this technology is that it is challenging to scan surfaces that are shiny or transparent [9]. It is also not the greatest 3D-imaging technology for capturing the texture of an object. This type of 3D-imaging is implemented in various types of design and it is usually used for short-range 3D-imaging of small objects. This technology is cheaper than the average CMM but still costly. The prices of laser triangulation 3D-scanners range between $2K and $100k dollars. Figure 3 shows two examples of 3D-scanners that use this 3D-imaging technology.

(a) Creaform HandySCAN handheld 3D laser scanner ($100K) [14].

(b) NextEngine 3D-scanner ULTRA HD that uses a turn table for the object ($2K) [15].

Figure 3: Examples of 3D-scanners that use the laser triangulation technology.

2.1.2.2 Structured-light

Another technology that obtains a digital 3D-model of an object without making contact with the object is structured-light 3D-imaging. This technology works by using white or blue LED projected light. It works by projecting a light pattern onto the object consisting of bars, blocks, or other shapes. By using one or multiple sensors that look at the edge of those patterns or structures, the 3D-shape of the object can be determined. This technology also uses the trigonometric triangulation method, like laser triangulation technology, to determine the distances and the shape of the object [7].

Blue LED projected light is known to give better results. It results in higher accuracy and minimizes the effect of reflections and transparency [16]. The reason that blue light works better is that it has a narrower wavelength. Due to this, it is more resistant to ambient light and results in very accurate and smooth data [9].

One main advantage of this 3D-imaging technology is that it can capture large areas of the object at once, resulting in a very fast scan. The scan can potentially be done in a few seconds. This technology also has the advantage that it can provide high accuracy and high resolution. It can provide accuracy as high as 10 microns and resolution as high as 16 microns [7]. It also can scan small objects and large objects. This technology also can capture the texture of the object. The price of the devices can vary from low-cost to expensive, depending on the accuracy and the resolution. Another advantage is that this technology can be fully automated. The devices using this technology can either be handheld or stationary devices. Stationary devices deliver result in accuracy and resolution [17].

One of the disadvantages of this technology is that it is sensitive to lighting effects and can have problems when working with bright light in outer space [18]. It also does not work optimally with shiny reflective, transparent, or black surfaces. This is because the light will be scattered or absorbed and alter the calculations for the scan [19]. Figure 4 shows two examples of devices that use the structured-light technology to create 3D-models.

(a) Go!Scan3D, white structured-light handheld 3D-scanner ($30K) [20].

(b) Polyga Compact L6, white structured-light stationary 3D-scanner ($16K) [21].

Figure 4: Examples of 3D-scanners that use the structured-light technology.

2.1.2.3 Time-of-flight

3D-scanners using the time-of-flight (TOF) technology can be divided into laser pulse-based TOF and laser phase-shift TOF. Laser pulse-based TOF is based on the fact that the speed of light is known very precisely. This means that if the amount of time needed for a laser to reach an object and reflect it back to the sensor is known, the distance can also be calculated from the sensor to the object. These systems using this technology are equipped with circuitry that is accurate to picoseconds. Millions of pulses of the laser return to the sensor and calculate the distances [7].

Laser phase-shift TOF conceptually works the same as laser pulse-based TOF. In addition to laser pulsing, laser phase-shift TOF also modulates the power of the laser beam. By doing this, the 3D-scanner compares the phase of the laser sent out and the phase of the laser returned to the sensor. Laser phase-shift TOF 3D-scanners are commonly more accurate than laser pulse-based TOF 3D-scanners. Although laser phase-shift TOF 3D-scanners are more accurate, they are less suitable for 3D-imaging objects at a long-range. Laser phase-shift TOF 3D-scanners are suitable for 3D-imaging objects in a range of 300m or less. Laser pulse-based 3D-scanners are good for imaging objects in a range of 1000m or less [7].

In general, the main advantage of TOF 3D-scanners is that they are suitable for long-range 3D-imaging and the 3D-imaging of large objects. They are also effective in producing images of objects in real-time, enabling the easy tracking of movement [22]. In addition, this technology has great automation possibilities.

One disadvantage of this technology is that it is a quite slow 3D-imaging technology. It requires multiple scans, limiting the speed of the 3D-imaging process. Another disadvantage is that it is not as accurate as laser triangulation 3D-scanners or structured-light 3D-scanners. Although the scanners contain highly accurate sensors, the accuracy of these devices is relatively low, ranging in centimeters. This is primarily a result of how the speed of light is affected by various factors, such as temperature and humidity. This 3D-imaging technology also cannot provide highly detailed textures of the 3D-scanned objects [8]. Figure 5 shows two examples of 3D-scanners that use TOF.

Figure 5: Velodyne HDL-32E TOF 3D-scanner ($8K) [23].

2.1.2.4 Photogrammetry

Another technology used to create 3D-models of objects is called photogrammetry. Photogrammetry is a three-dimensional coordinate measuring technology that uses photographs as the fundamental medium for metrology or measurement. The fundamental principle used in photogrammetry is triangulation. It is done by taking photographs of the object from at least two different positions. By doing this, 'lines of sight' can be developed from each camera position to points on the object. These lines of sight, sometimes called rays owing to their optical nature, are mathematically intersected with software to produce the three-dimensional coordinates of the points of interest [24]. As a result, a digital 3D-model can be constructed from the calculation of the three-dimensional coordinates of the points.

The main advantage of photogrammetry is its capability of capturing the texture and full color of an object in a highly detailed manner [25] [26]. Therefore, this technology is being embraced by the archaeological community because it allows for digital documentation of artefacts with more realistic textures [27]. It is also more preferred because it is a lower-cost option compared to other technologies. Great levels of accuracy and resolution can be achieved with photogrammetry. Another advantage of photogrammetry is that it can be used for large objects but also for smaller objects [18] [26]. Photogrammetry also has good automation possibilities.

One of the disadvantages with this technology is that the post-processing of the photographs with the photogrammetry software can be a time-consuming process [28]. Photogrammetry can be a very quick technology to acquire digital 3D-models of objects, but therefore a powerful computer is needed to run photogrammetry algorithms [22]. Comparing to for example structured-light 3D-imaging, which can create a 3D-scan in seconds, photogrammetry is a slower technology. Another disadvantage is that the accuracy and resolution of the 3D-model are very much dependent on the quality of the photographs. Photographs with poor resolution will produce low-quality scans with mesh holes [22]. One more disadvantage is the reduced depth of field experienced in the acquisition of photographs of the object [29]. This results in photographs where the object is not completely in focus, thus not resulting in an optimal data set to use as an input for the photogrammetry software. Another disadvantage is that it has difficulty with transparent and shiny surfaces. It also has difficulties with smooth, flat, or solid-colored surfaces [26]. In Figure 6 an example of a photogrammetric system is shown.

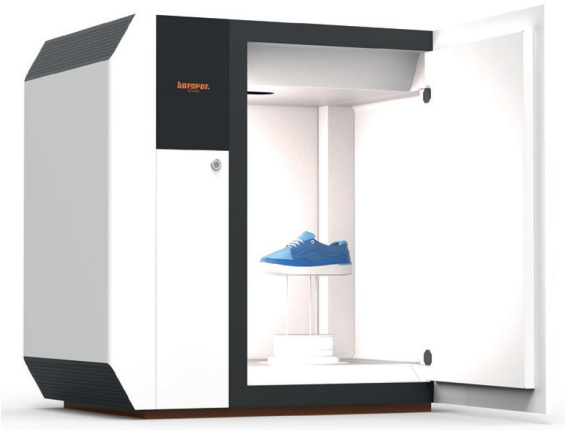

Figure 6: Botscan MOMENTUM that utilizes photogrammetry to create 3D-models ($50K) [30].

2.2 Summary and evaluation

The existing 3D-imaging technologies with their available 3D-imaging devices and applications have been discussed and compared. The most important criteria to evaluate the different 3D-imaging technologies that have been assessed are the following: the scale of the object on which the 3D-imaging technology can be performed, the quality of the texture, the time required to do the 3D-scan, the cost involved, the automation possibility, the accuracy and resolution, and the complexity involved in using the 3D-imaging technology.

Photogrammetry has shown to be the most suitable technology to create a digital 3D-model of an object for the chosen application. Photogrammetry has the capability to make 3D-models of small objects with full color and realistic texture. It also has the possibility to be automated and can be a cost-effective technology to obtain 3D-models compared with other technologies. In the next chapter, photogrammetry and the systems using this technology will be addressed more in detail.

3 Close-range photogrammetry

In this chapter, close-range photogrammetry will be studied more in detail. The goal is to understand the working principle and to map all the important requirements to optimally use close-range photogrammetry. The existing literature about using close-range photogrammetry for small objects and existing systems will be studied to identify a knowledge gap.

3.1 Working principle

As mentioned earlier, photogrammetry creates digital 3D-images of objects by taking multiple photographs at different angles from the object. These photographs are then used as a data set to implement in photogrammetry software that creates a 3D-image. The photogrammetry software identifies identical feature points between the different photographs to calculate the distances and creates a 3D-image of the object. In Figure 7 this process is depicted. More information on the exact calculations involved in close-range photogrammetry can be found in the book Close Range Photogrammetry And 3D-Imaging [31].

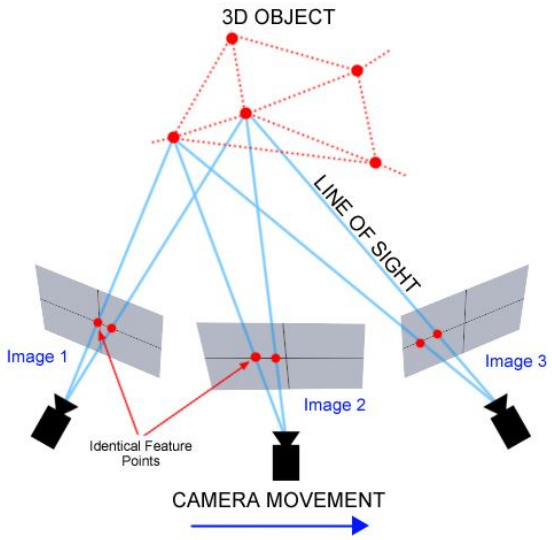

Figure 7: Photogrammetric procedure for calculating the shape of the object. By obtaining several images of the object, identical feature points can be recognized by the photogrammetry software, and the three-dimensional coordinates of the object can be calculated [32].

3.2 Requirements for close-range photogrammetry

To create an optimal data-set of photographs that is going to be used as an input for the photogrammetry software, the following requirements have to be met [31] [33]:

- **High-resolution:** The photographs have to be high-resolution, with the object as much in focus as possible. This is because the resulting 3D-image is very much dependent of the resolution of the photographs. High-resolution photographs are desired to capture the details of the texture as much as possible in the digital 3D-image.
- **Depth of field:** Sufficient depth of field is needed to capture the object completely in focus. Small depth of field results in blurry photographs, diminishing the quality of the 3D-image.
- **Lighting:** Good lighting should be applied to the scene of the object. Good lighting means that no strong shadows and no strong reflections are observed which could diminish the quality of the 3D-image. Identical feature points are harder for the software to identify when strong shadows and strong reflections are present.
- **Sufficient angles photographed:** The photographs should be taken from a sufficient amount

of different angles of the object. This is self-explanatory, this is necessary in order to capture the object completely in the 3D-image.

- **Sufficient overlap between the photographs:** As explained in Section 3.1, in order for the photogrammetry software to recognize identical feature points, the photographs should have sufficient overlap.

3.3 Available software for close-range photogrammetry

Photogrammetry software is available in different forms [34]. Photogrammetry software exists for long-range photogrammetry and close-range photogrammetry. One example of long-range is aerial photogrammetry. An example of close-range photogrammetry is photogrammetry applied for small objects. Some of the software can create 3D-images for long-range photogrammetry and close-range photogrammetry. And some of the software available can only be used for long-range photogrammetry or close-range photogrammetry. Although there is a wide variety of photogrammetry software available with each its strengths and limitations, some of them are popular and used extensively. One of them is Agisoft Metashape, which is highly favored in the highly competitive photogrammetric software industry. Agisoft Metashape is widely used due to its quality, processing time, and reduced complexity which is important for non-experts in photogrammetry [35].

3.4 Automation possibilities with close-range photogrammetry

A major weakness of photogrammetry is the dependence of a specialized camera operator who can configure the camera parameters and obtain the photographs in the right way. If the images are not acquired correctly, subsequent 3D reconstruction will be affect by the presence of significant noise and construction errors [36]. If the process is not automated it allows for more user error, so the quality of the 3D-model depends greatly on the experience of the operator [27]. Therefore, it is desirable to automate the image acquisition to create an optimal data-set to implement in the photogrammetry software. The automation of this image acquisition is possible to achieve and has been done. Existing designs have shown that it can be automated to a great extent. The acquisition of photographs can be automated with a system that takes photos of the object at different angles. The camera path is well defined and the location of the object is known or fixed. These photos have to be imported into the photogrammetry software to create a 3D-model. This so-called post-processing is harder to automate, but it still possible. In the next section the existing designs for obtaining photographs for photogrammetry will be discussed.

3.5 Available knowledge and existing devices using close-range photogrammetry

In Section 2.1.2.4 one existing device using close-range photogrammetry was shown. This device costs \$50K, which is quite expensive. Cheaper alternatives have been designed and proven to create 3D-models of good quality. In Figure 8 two examples are shown by the company Openscan. These low-cost photogrammetric systems are designed with 3D-printable parts, stepper motors, raspberry pi cameras, and arduinos to keep the cost low.

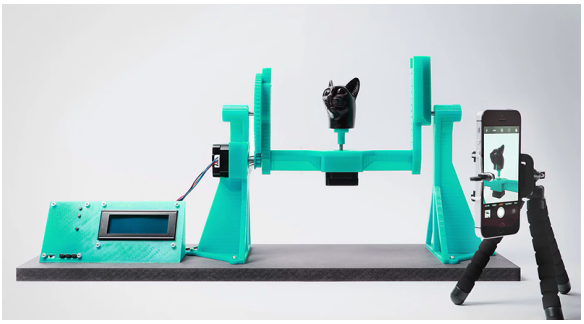

(a) Openscan 3D-scanner [37].

(b) Openscan 3D-scanner [37].

Figure 8: Examples of low-cost photogrammetric systems by the company Openscan [37].

In literature different designs can be found for specifically the creation of 3D-models for archaeological artifacts. One example is shown in Figure **??**. This design has the ability to create good quality 3D-models of archaeological artifacts with a relatively low-cost system. It works with stepper motors to move the object and the camera.

The mentioned existing designs found in the literature, however, could be improved. In the scientific results of different papers it has been discussed that a small depth of field results in lower quality 3D-models [38]. As mentioned before, the quality of the constructed 3D-models is highly dependent on the quality of the photographs. The existing devices take one photo at each angle of the object. There are two reasons why this would not give the best result. The first reason is, by only taking one photo at a close distance, only a specific part of the object is in focus due to a small depth of field. This photo will then be used in the photogrammetry software and the part of the object that is out of focus will not be modelled with a highly detailed texture in 3D. The second reason is, by taking a photo of the object at a relatively larger distance, the object can be completely in focus, but there is a loss in resolution. This is because the resolution of the image sensor is not completely utilized. A higher quality 3D-model could be achieved where there is a more detailed texture on the 3D-model. This could be done by solving the small depth of field problem when taking a photo at a close distance relative to the object. A possible solution is using macro-photography in combination with focus stacking. In the following chapter these techniques will be discussed and how they could potentially be combined with photogrammetry and implemented in a cost-effective automated system. Also, in present literature different important aspect cannot be found regarding close-range photogrammetry for archaeological artefacts. These aspects include: optimal lightning, optimal overlap, setting of the object, optimal trajectories of taking photographs, focus stacking, and speed limitations. This presents a research opportunity.

4 Macro-photography and focus stacking

As discussed in the previous chapter, macro-photography in combination with focus stacking could provide an improvement in the quality of the 3D-model of archaeological artefacts and other small objects. In the following sections, macro-photogrammetry and focus stacking will be discussed. Then it will be explained how focus stacking could be implemented in photogrammetry. Finally, existing results and systems will be analyzed that have implemented this.

4.1 Macro-photography and focus stacking

Macro-photography is close-up photography of small subjects, with the intention of depicting them as large as possible, so that details of the texture become visible [39]. With this photography technique, a small depth of field is a problem that occurs. The reason for that is the very nature of optics: the closer a subject is to the lens, the shallower the depth of field is going to be. This can be counteracted by a narrow aperture, which cancels out a large portion of the light cone in order to decrease the fall-off in sharpness. But this only works to a certain degree. If the aperture opening becomes too narrow, light waves begin to bend and soften the image. This phenomenon is called diffraction [40]. Therefore, it is desired to use a different technique to extend the depth of field. There are different techniques to extend the depth of field and one of them is called focus stacking. Focus stacking is combining several photographs of the object where different parts of the object are in focus. By doing this, a full in-focus image can be created of the object. There exists different software that achieves focus stacking. Some of the focus stacking software that are available are: Helicon Focus, Picolay, Combine ZP, and others. In Figure 9 the working principle of focus stacking is shown.

Figure 9: Working principle of focus stacking. In the left image, the front of the fly is in focus. In the middle image, the back of the fly is in focus. By combining these images, a full in-focus image of the fly can be created which is shown on the right [41].

4.2 Combining focus stacking with photogrammetry

Focus stacking can be achieved in different ways. One way is by moving the camera with a fixed focal length in several steps. At each step, a photograph is taken where a part of the object is in focus. This is repeated until the complete object has been photographed. Another way to achieve focus stacking is by controlling the camera with software. By changing the focus point and taking photographs with different focus points on the object a set of images can be created that can be stacked. These different ways of achieving focus stacking to create a full in-focus image of the object could be combined with photogrammetry. A system could be designed where the object is photographed from different angles. At each angle, the object is photographed closely multiple times with different parts of the object in focus. These photographs at each angle can then be stacked and implemented in the photogrammetry software. Combining focus stacking with photogrammetry presents an opportunity to create a higher quality data set.

4.3 Existing systems combining focus stacking with photogrammetry

In literature, only one system can be found that uses focus stacking in combination with photogrammetry. In the paper, it is mentioned that they believe that they are the first in designing such a system. A system for automated multi-view extended depth of field imaging [42]. This system is intended for the 3D-modelling of insects. So, it cannot be used for the digitization of archaeological artefacts. In Figure 10 the system can be seen.

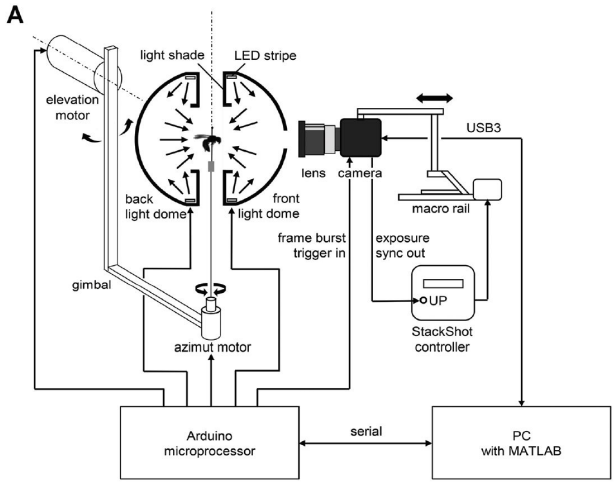

(a) Schematic setup of the system [42].

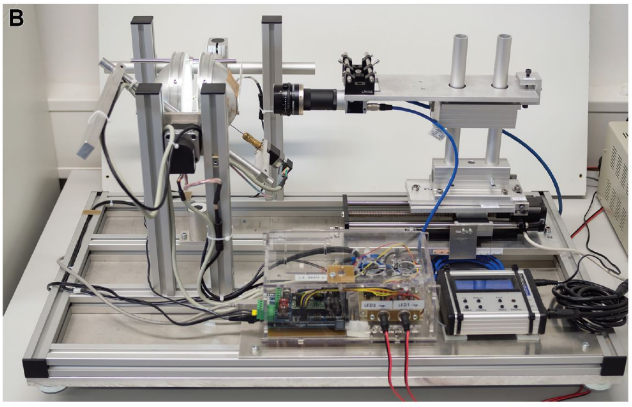

(b) Real life setup of the system [42].

Figure 10: Schematic setup of the system and the system depicted that uses automated multi-view extended depth of field imaging for photogrammetry [42].

In the works of others, it has been shown that creating 3D-models of archaeological artefacts with photogrammetry in combination with focus stacking resulted in higher quality 3D-models [43] [44]. In literature, a system that automates the acquisition of photographs for photogrammetry in combination with focus stacking cannot be found for the 3D-modelling of archaeological artefacts. This presents an opportunity to design such a system and to investigate what aspects are important in designing it.

5 Discussion

In this literature review, state-of-the-art 3D-scanning technologies have been studied. Each 3D-scanning technology presented its own advantages and limitations, and each 3D-scanning technology has shown to have its applications. The objective was to identify which one of these technologies is the most suitable to create high-quality 3D-models of archaeological artefacts. With high-quality 3D-models is meant a technology that can capture the colors and texture of the object with high detail.

During this research into the existing 3D-scanning technologies, a technology was found that is suitable for 3D-modelling archaeological artefacts. The technique found is called photogrammetry. Photogrammetry presents an opportunity to create 3D-models of objects while capturing the texture of the object in a highly detailed manner. Photogrammetry has shown to be the most suitable technology to create a digital 3D-model of archaeological artefacts. Photogrammetry can make 3D-models of small objects with full color and realistic texture. It also can be automated and can be a cost-effective technology to obtain 3D-models compared with other technologies.

Close-range photogrammetry has been studied more in detail to understand the working principle and to map all the important requirements to optimally use close-range photogrammetry. The existing literature about using close-range photogrammetry for small objects and existing systems were studied. The requirements have been identified to create an optimal data set for photogrammetry. Also, a possible improvement in existing designs has been identified and research possibilities have arisen. Shallow depth of field is a reoccurring problem in the 3D-modelling of small objects by using photogrammetry. Focus stacking could provide a solution, where multiple images of the object are stacked together to create a full-in-focus image of the object. Focus stacking could be combined with photogrammetry to create an automated system to acquire photographs of an object. Successfully doing this will result in higher-quality 3D-models of archaeological artefacts.

6 Conclusion

After the conduction of this literature review, a suitable technique was found to create high-quality 3D-models of archaeological artefacts. The technique found is called photogrammetry, and its main advantage is that it can create 3D-models with full color and realistic texture. Close-range photogrammetry has been studied further in detail. A possible improvement and knowledge gap was found. A proposal is made to create a system to automate the acquisition of photographs of archaeological artefacts and implementing focus stacking. Successfully creating this system and researching the aspects involved will result in higher-quality 3D-models of archaeological artefacts. By doing so, the 3D-digitisation of archaeological artefacts can be improved, which serves different purposes.

References

[1] P. Santos, M. Ritz, C. Fuhrmann, R. Monroy, H. Schmedt, R. Tausch, M. Domajnko, M. Knuth, and D. Fellner, Acceleration of 3D Mass Digitization Processes: Recent Advances and Challenges, 04 2017, pp. 99–128.

[2] The Den Foundation, "Busines model innovation cultural heritage," 2010.

[3] Sculpteo, "How does 3d scanning work?" 2019.

[4] Revopoint, "An introduction of 3d scanning and 3d scanners," 2019.

[5] Edge 3D Technologies, "3d scanning: Methods, applications and advantages," 2019.

[6] CMM Solutions, "Fifty years of cmm history leading up to a measuring revolution," 2019.

[7] EMS-USA, "Types of 3d scanners and 3d scanning technologies," 2018.

[8] NeoMetrix Technologies, "A guide to 3d scanners," 2017.

[9] Capture3D, "3d scanning definitive guide," 2019.

[10] Engineering.com, "3 tips for choosing the best coordinate measuring machine for your quality process," 2016.

[11] FOX VALLEY METROLOGY, "Wenzel lh 1210 coordinate measuring machine," 2020.

[12] Nikon, "Nikon metrology presents the premium, portable cmm – mcax articulated arm with mmdx laser scanner," 2012.

[13] 3DSYSTEMS, "A guide to 3d scanner technology," 2019.

[14] GoEngineer, "Creaform handyscan, high resolution portable 3d scanning," 2020.

[15] NextEngine, "Next engine 3d scanner," 2020.

[16] 3D Insider, "Structured light 3d scanning: What is it and how does it work?" 2020.

[17] Polyga, "What are the advantages of using a structured-light 3d scanner?" 2020.

[18] Pick 3D Printer, "What is a 3d scanning – how does 3d scanning work?" 2020.

[19] 3SPACE, "White light vs. blue light 3d scanning," 2019.

[20] CREAFORM, "Go!scan 3d - the fastest and easiest 3d scanning experience," 2020.

[21] Polyga, "Polyga compact l6," 2020.

[22] 3DCompare, "3d scanning," 2020.

[23] Velodyne Lidar, "Hdl-32e, high resolution real-time 3d lidar sensor," 2020.

[24] Jay A. Siegel, Pekka J. Saukko and Max M. Houck, "Encyclopedia of forensic sciences," 2013.

[25] Techmed3D, "Photogrammetry vs. 3d scanning," 2019.

[26] Photomodeler Technologies, "Photogrammetry vs 3d scanning," 2020.

[27] Lanmar Services, "Laser scanning vs. photogrammetry," 2014.

[28] 3DInsider, "Types of 3d scanning technologies," 2019.

[29] Novuslight, "Pros and cons of popular 3d technologies," 2019.

[30] Botspot, "Botscan momentum," 2020.

[31] T. Luhmann, S. Robson, S. Kyle, and J. Boehm, Close-Range Photogrammetry and 3D Imaging. Berlin, Boston: De Gruyter, 18 Nov. 2019. [Online]. Available: https://www.degruyter.com/view/title/539949

[32] The Haskins Society, "Making 3d models with photogrammetrybotscan momentum," 2020.

[33] Agisoft, "Agisoft user manuals," 2020.

[34] All3DP, "2020 best photogrammetry software," 2020.

[35] Cultural Heritage Imaging, "Photogrammetry," 2020.

[36] M. Rodríguez Martín and P. Rodríguez-Gonzálvez, "Suitability of automatic photogrammetric reconstruction configurations for small archaeological remains," Sensors, vol. 20, p. 2936, 05 2020.

[37] Openscan, "From object to 3d-model," 2020.

[38] C. Nicolae, E. Nocerino, F. Menna, and F. Remondino, "Photogrammetry applied to problematic artefacts," vol. XL-5, 06 2014.

[39] Photographylife, "Everything you need to know about macro photography," 2019.

[40] Petapixel, "Beginner's guide to focus stacking for macro photography," 2019.

[41] Wikipedia, "Focus stacking," 2020.

[42] B. Ströbel, S. Schmelzle, N. Blüthgen, and M. Heethoff, "An automated device for the digitization and 3d modelling of insects, combining extended-depth-of-field and all-side multi-view imaging," ZooKeys, vol. 759, pp. 1–27, 2018. [Online]. Available: https://doi.org/10.3897/zookeys.759.24584

[43] Hellberg Photo, "Photogrammetry - using stacked pictures," 2019.

[44] G. P. W. Lauras, "Automação de processo de digitalização fotogramétrica para medição mecânica não-destrutiva de amostras pequenas," Ph.D. dissertation, Universidade Federal do Rio de Janeiro, 2020.

B

Python code

```
from time import sleep
import RPi.GPIO as GPIO
from picamera import PiCamera
import os
import subprocess

camera = PiCamera()
camera.resolution = (4056, 3040)
camera.start_preview() # Show live view of RPi HQ Camera
sleep(5)

# GPIO Pins

DIR1 = 9  # Direction GPIO Pin
STEP1 = 25  # Step GPIO Pin

DIR2 = 18  # Direction GPIO Pin
STEP2 = 27  # Step GPIO Pin

DIR3 = 2  # Direction GPIO Pin
STEP3 = 3  # Step GPIO Pin

# Mode Pins (Microstep Resolution GPIO Pins)

MODE1 = (0, 7, 8)
MODE2 = (10, 24, 23)
MODE3 = (17, 15, 14)

# GPIO Setup

GPIO.setmode(GPIO.BCM)
GPIO.setwarnings(False)

GPIO.setup(DIR1, GPIO.OUT)
GPIO.setup(STEP1, GPIO.OUT)
GPIO.setup(MODE1, GPIO.OUT)

GPIO.setup(DIR2, GPIO.OUT)
GPIO.setup(STEP2, GPIO.OUT)
GPIO.setup(MODE2, GPIO.OUT)

GPIO.setup(DIR3, GPIO.OUT)
GPIO.setup(STEP3, GPIO.OUT)
GPIO.setup(MODE3, GPIO.OUT)

# General

CW = 1  # Clockwise Rotation
CCW = 0  # Counterclockwise Rotation

```

```
# Steps Per Revolution (360/1.8/microstepping resolution)

SPR3 = 25600

# Microstepping Resolution Settings

RESOLUTION = {'Full': (0, 0, 0),
              'Half': (1, 0, 0),
              '1/4': (0, 1, 0),
              '1/8': (1, 1, 0),
              '1/16': (0, 0, 1),
              '1/32': (1, 0, 1)}

# Stepper Resolutions

GPIO.output(MODE1, RESOLUTION['1/32'])  # Stepper 1 (Turntable)
GPIO.output(MODE2, RESOLUTION['Half'])  # Stepper 2 (Camera Mover)
GPIO.output(MODE3, RESOLUTION['Half'])  # Stepper 3 (Tilt Mechanism)

# Delay between steps for all 3 stepper motors

delay1 = 0.0004
delay2 = 0.00015
delay3 = 0.00013

# Movement

Depth_Of_Field = 5  # In mm
Rev_FS = Depth_Of_Field/2  # Amount of revolutions needed with the leadscrew
Stepsize_FS = int(Rev_FS*SPR2)  # Steps for each focus stacking step

Y = 10 # Amount of steps for focus stacking

# Calculte the amount of steps the stepper motor has to move to return to the original
    position:
Steps_Back_FS = Y*Stepsize_FS

# Amount of position on the turntable (determines photograph overlap)
X = 40

Steps_Turntable = 160 # Amount of steps for one revolution divided by X

# Preliminaries for the loop.
stepsize_tilt_0=SPR3
stepsize_tilt=SPR3

# Loop repeats X Times, which is the amount of times required for the turntable to turn 360
    degrees:

Tilt_positions = 1
na = 0
for p in range(Tilt_positions):

    for a in range(X):
        # Make new folder X for stack 1
        # For each step in X, a new folder is created with a new name. For example 'Stack 1'.
        dirloc = f'/media/pi/DELLUSB/RPi_Photographs/Scan_1/Stack_{na}'
        os.mkdir(dirloc)

        # Stepper 2 (Camera Mover) moves Y steps

        camera.capture(f'/media/pi/DELLUSB/RPi_Photographs/Scan_1/Stack_{na}/photograph_{0}.
    jpg')
        #cmd = "raspistill -t 2000 -o "f'/media/pi/DELLUSB/RPi_Photographs/Scan_1/Stack_{na}/
    photograph_{0}.jpg'""
        #subprocess.call(cmd, shell=True)

        for b in range(Y):

            # Stepper 2 (Camera Mover) movement
            GPIO.output(DIR2, CCW)
```

```
118
119             for c in range(Stepsize_FS):
120                 GPIO.output(STEP2, GPIO.HIGH)
121                 sleep(delay2)
122                 GPIO.output(STEP2, GPIO.LOW)
123                 sleep(delay2)
124
125             sleep(1)
126
127             # Make photograph while sleep
128             # Save photograph in corresponding folder
129
130             camera.capture(f'/media/pi/DELLUSB/RPi_Photographs/Scan_1/Stack_{na}/photograph_{
    b+1}.jpg')
131
132             #cmd = "raspistill -t 2000 -o "f'/media/pi/DELLUSB/RPi_Photographs/Scan_1/Stack_{
    na}/photograph_{b+1}.jpg'""
133             #subprocess.call(cmd, shell=True)
134
135
136         # Stepper 2 (Camera Mover) moves back to the original position
137         GPIO.output(DIR2, CW)
138
139         for d in range(Steps_Back_FS):
140             GPIO.output(STEP2, GPIO.HIGH)
141             sleep(delay2)
142             GPIO.output(STEP2, GPIO.LOW)
143             sleep(delay2)
144
145         sleep(1)
146
147         # Stepper 1 (Turntable) Movement
148
149         GPIO.output(DIR1, CW)
150
151         for e in range(Steps_Turntable):
152
153             GPIO.output(STEP1, GPIO.HIGH)
154             sleep(delay1)
155             GPIO.output(STEP1, GPIO.LOW)
156             sleep(delay1)
157
158         sleep(1)
159         na = na+1
160
161     # Stepper 3 (Tilt Mechanism) movement
162     # Mechanism is tilted and then the loop is repeated to make photographs
163
164     GPIO.output(DIR3, CCW)
165
166     if Tilt_positions > 1:
167         stepsize_tilt = int(stepsize_tilt_0/(Tilt_positions-1))
168
169     if Tilt_positions != 1 and p != (Tilt_positions-1):
170
171         for f in range(stepsize_tilt):
172             GPIO.output(STEP3, GPIO.HIGH)
173             sleep(delay3)
174             GPIO.output(STEP3, GPIO.LOW)
175             sleep(delay3)
176
177     sleep(1)
178
179 if Tilt_positions > 1:
180
181     GPIO.output(DIR3, CW)
182     for f in range(stepsize_tilt_0):
183         GPIO.output(STEP3, GPIO.HIGH)
184         sleep(delay3)
185         GPIO.output(STEP3, GPIO.LOW)
186         sleep(delay3)
```

```
187
188 camera.stop_preview()
```

Bibliography

[1] 3dprint.com. Properties of 3d-printed pla, 2021.

[2] Adafruit. Crop factor, 2021. URL https://learn.adafruit.com/raspberry-pi-hq-camera-lenses/crop-factor.

[3] Agisoft. Agisoft user manuals. 2020.

[4] All3DP. 2020 best photogrammetry software. 2020.

[5] Artifacts Encylopedie. Small archaeological artifacts. 2021.

[6] Botspot. Botscan momentum. 2020.

[7] Cultural Heritage Imaging. Photogrammetry. 2020.

[8] Daycounter. Stepper motor calculations. 2021.

[9] Fixthephoto.com. Best focus stacking software, 2021.

[10] Jay A. Siegel, Pekka J. Saukko and Max M. Houck. Encyclopedia of forensic sciences. 2013.

[11] Lanmar Services. Laser scanning vs. photogrammetry. 2014.

[12] Led-Proffesional. Light emitting diode spectrum, 2021.

[13] Thomas Luhmann, Stuart Robson, Stephen Kyle, and Jan Boehm. *Close-Range Photogrammetry and 3D Imaging*. De Gruyter, Berlin, Boston, 18 Nov. 2019. ISBN 978-3-11-060725-3. doi: https://doi.org/10.1515/9783110607253. URL https://www.degruyter.com/view/title/539949.

[14] Lumenlearning. Combined focal length equations, 2021. URL https://courses.lumenlearning.com/boundless-physics/chapter/lenses/#:~:text=If%20the%20lenses%20of%20focal,d%20f%201%20f%202%20.

[15] Machinedesign. The difference between servo and stepper motors, 2021. URL https://www.machinedesign.com/mechanical-motion-systems/article/21836868/whats-the-difference-between-servo-and-stepper-motors.

[16] Corina Nicolae, Erica Nocerino, Fabio Menna, and Fabio Remondino. Photogrammetry applied to problematic artefacts. volume XL-5, 06 2014. doi: 10.5194/isprsarchives-XL-5-451-2014.

[17] Pcblinear. Leadscrew or belt drives, 2021. URL https://www.pbclinear.com/Blog/2020/February/Lead-Screw-or-Belt-Drives.

[18] Petapixel. Beginner's guide to focus stacking for macro photography. 2019.

[19] Pololu. Drv8825 stepper motor driver carrier, high current, 2021. URL https://www.pololu.com/product/2133.

[20] Manuel Rodríguez Martín and Pablo Rodríguez-Gonzálvez. Suitability of automatic photogrammetric reconstruction configurations for small archaeological remains. *Sensors*, 20:2936, 05 2020. doi: 10.3390/s20102936.

[21] Pedro Santos, Martin Ritz, Constanze Fuhrmann, Rafael Monroy, Hendrik Schmedt, Reimar Tausch, Matevz Domajnko, Martin Knuth, and Dieter Fellner. *Acceleration of 3D Mass Digitization Processes: Recent Advances and Challenges*, pages 99–128. 04 2017. ISBN 978-3-319-49606-1. doi: 10.1007/978-3-319-49607-8_4.

[22] Seeedstudio. Crop factor effects, 2021. URL https://www.seeedstudio.com/blog/2020/06/15/how-does-crop-factor-affect-raspberry-pi-camera-lenses-m/.

[23] Bernhard Ströbel, Sebastian Schmelzle, Nico Blüthgen, and Michael Heethoff. An automated device for the digitization and 3d modelling of insects, combining extended-depth-of-field and all-side multi-view imaging. *ZooKeys*, 759:1–27, 2018. ISSN 1313-2989. doi: 10.3897/zookeys.759.24584. URL https://doi.org/10.3897/zookeys.759.24584.

[24] The Den Foundation. Busines model innovation cultural heritage. 2010.

[25] The Haskins Society. Making 3d models with photogrammetrybotscan momentum. 2020.

[26] Wencheng Wang and Faliang Chang. A multi-focus image fusion method based on laplacian pyramid. *JCP*, 6:2559–2566, 12 2011. doi: 10.4304/jcp.6.12.2559-2566.

[27] Wikipedia. Leadscrew. 2021.

[28] Wikipedia. Depth of field, 2021. URL https://en.wikipedia.org/wiki/Depth_of_field.

[29] Wikipedia. Light emitting diode, 2021. URL https://en.wikipedia.org/wiki/Light-emitting_diode.

[30] Wikipedia. Leadscrew mechanics, 2021.